Chapter 14
Regular Structures with Random Interactions: A New Paradigm

14.1 Introduction

Embedded random matrix ensembles opened up a new paradigm of regular structures with random interactions in isolated finite quantum systems. For the first time in 1998, Johnson, Bertsch and Dean, using the nuclear shell model, noticed that random two-body interactions lead to ground states, for even-even nuclei, having spin 0^+ with very high probability [1]. Similarly, Bijker and Frank [2] using interacting boson model of atomic nuclei found that random interactions generate vibrational and rotational structures with high probability. Examples are shown in Figs. 14.1 and 14.2 and Table 14.1. Later studies in nuclear structure with random interactions revealed statistical predominance of odd-even staggering in binding energies, the seniority pairing gap and 0^+, 2^+, 4^+, ... yrast sequence. Also seen are regularities in parity distributions in ground states of even-even, odd-A and odd-odd nuclei, in energy centroids, spectral variances and in many other quantities. On the other hand it is also found that random interactions generate, for systems with even number of fermions, spin zero ground states preferentially (see the discussion in Sect. 7.1.1 and Fig. 7.2) giving rise to delay in Stoner instability in itinerant systems and odd-even staggering in ground state energies in nm scale metallic grains (see the discussion in Sect. 7.1.2 and Figs. 7.3 and 7.4). The result that regular features can arise due to random interactions (with rotational and other symmetries) is opposed to the conventional ideas of using regular (or coherent) interactions like pairing in understanding the structure of nuclear and other systems. As Zelevinsky and Volya state [3], this is not limited to nuclear physics. Atomic clusters, particles in traps, quantum dots, disordered systems such as quantum spin glasses, are just a few examples where the same questions are to be answered—to what extent a realistic interaction can be random but still give the ground state and the levels near the yrast line to be realistic? References [3, 4] give early reviews on the topic of regular structures from random interactions.

V.K.B. Kota, *Embedded Random Matrix Ensembles in Quantum Physics*,
Lecture Notes in Physics 884, DOI 10.1007/978-3-319-04567-2_14,

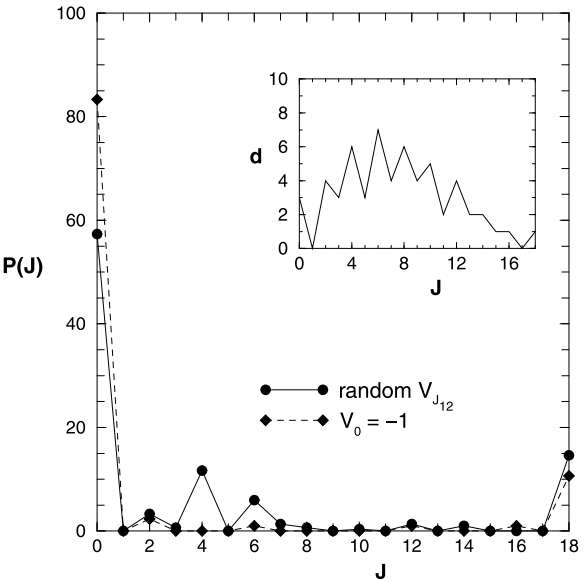

Fig. 14.1 Probability for spin-0 ground states for $(\frac{11}{2})^{m=6}$ system. Calculations use 1000 samples of random interactions preserving J, i.e. EGOE(2)-$(j = \frac{11}{2} : J)$ is used with 1000 members. Results obtained by putting $V_0 = -1$ (rest of the $V_{J_{12}}$ being Gaussian random variables) are also shown in the figure (results obtained by putting $V_0 = 0$ are almost same as those given by random interactions). In addition, the matrix dimensions $d(m = 6, J)$ are also shown in the insect figure. Figure is constructed using the results in [5]

Large number of numerical calculations for many particle systems are carried out using nuclear shell model, fermions in a single-j shell or two-j shells, bosons in a single ℓ orbit and interacting boson models (IBMs) for nuclei and molecules (spIBM, sdIBM, sdgIBM etc.) using ensembles of random interactions. For the preponderance of $J^\pi = 0^+$ states in even-even nuclei: (i) Zelevinsky and Volya [3] proposed the idea of 'geometric chaos' as the source of regularities seen in nuclear shell model results; (ii) Zhao et al. [4] proposed a empirical rule for describing the results for $(j)^m$ fermion and $(\ell)^m$ boson systems with extensions to more complicated systems; (iii) Papenbrock and Weidenmüller [6] proposed an explanation in terms of fixed-J spectral variances. On the other hand Kusnezov [7] showed that an approach based on random polynomials will apply if the H matrix is tridiagonal with analytical forms for the diagonal and the off-diagonal matrix elements known. This method is used to describe, completely analytically, the results for spIBM. Similarly, Bijker and Frank [8] employed mean-field methods for near quantitative understanding of the results for spIBM and sdIBM. The mean-field approach has been generalized to IBMs for two-level systems (with degeneracies n_1 and n_2 respectively) with $SO(n_1) \oplus SO(n_2)$ symmetry by Kota [9]. Similarly, regularities in energy centroids and spectral variances defined over symmetry subspaces generated by nuclear shell model and IBMs have been studied in a number of examples using trace propagation formulas. These group theoretical examples opened a new window to the study of regularities of many-body systems in the presence of random forces. We will now describe in this chapter these and other results on regularities generated by random interactions.

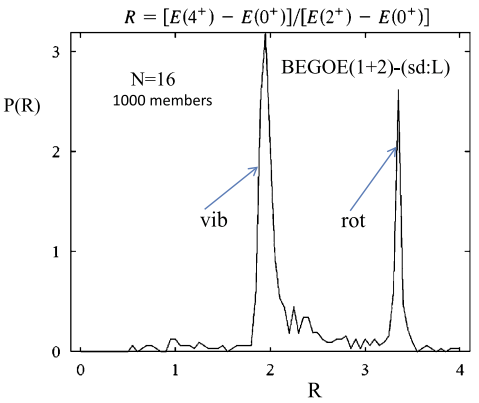

Fig. 14.2 Probability distribution $P(R)$ for the ratio $[E(4^+) - E(2^+)]/[E(2^+) - E(0^+)]$ with $\int P(R)dR = 1$ for a 1000 member BEGOE$(1+2)$-$(sd:L)$ for $m = 16$ bosons, i.e. for a 16 boson system in sdIBM with random one plus two-body interactions. Results in the figure clearly show that most members are either vibrational $[P(R) \sim 2]$ or rotational $[P(R) \sim 3.33]$. In the calculations, $P(R)$ is used for those members that gave $L = 0^+$ ground states. Figure is taken from [2] with permission from American Physical Society (Color figure online)

Table 14.1 Probabilities for ground states with $J^\pi = 0^+$ generated by random interactions in some $(2s1d)$ and $(2p1f)$ shell nuclei. Results are shown for EGOE(2)-J and its modifications as described in Sect. 14.2. Last column gives the percentage of 0^+ states in the model space and this is denoted by $d(0)/d$ in the table. All numbers in the table are in (%). Table is taken from [4]. See Sect. 14.2 for more details

Nuclei	EGOE(2)-J	RQE	RQE-NP	RQE-SPE	$d(0)/d$
^{20}O	50	68	50	49	11.1
^{22}O	71	72	68	77	9.8
^{24}O	55	66	51	78	11.1
^{44}Ca	41	70	46	70	5
^{46}Ca	56	76	59	74	3.5
^{48}Ca	58	72	53	71	2.9

14.2 Basic Shell Model and IBM Results for Regular Structures

Johnson et al. [1] considered examples of even-even nuclei in $(2s1d)$-shell with nucleons in $^1d_{5/2}$, $^2s_{1/2}$ and $^1d_{3/2}$ orbits with 63 independent TBME. Generating 1000 random interactions in this space, they have constructed Hamiltonian matrices for all allowed J values in many nucleon spaces using nuclear shell model codes. Using these, they have calculated the probability for the ground state to be $J^\pi = 0^+$. They have used EGOE(2)-J with degenerate sp energies for the three sp orbits. In addition, used are also three modified versions of EGOE(2)-J. One of them is with variance (v^2) of the two-particle matrix elements to be dependent on the two particle J_{12} and T_{12} values with $v^2(V^{J_{12},T_{12}}) = 1/[(2J_{12}+1)(2T_{12}+1)]$ as given by

particle-hole symmetry. This is called random quasi-particle ensemble (RQE). The other two are RQE without monopole pairing part (called RQE-NP) and RQE with non degenerate sp energies (call RQE-SPE). All the calculations are also repeated for some examples in $(2p1f)$-shell with nucleons in ${}^1f_{7/2}$, ${}^2p_{3/2}$, ${}^2p_{1/2}$ and ${}^1f_{5/2}$ orbits with 195 independent TBME. Results of this study are shown in Table 14.1. It is seen that 0^+ gs appears with probability ∼40–70 % although the fraction of 0^+ states in the total space is less than 12 % in all the examples. Several other shell model examples have been given by Zelevinsky et al. with similar results [3]. Extensive analysis using fermions in one and two j-orbits and similarly bosons in a single ℓ-orbit, sp orbits (i.e. spIBM), sd orbits and sdg orbits have been carried out by Zhao et al. [4] and Zelevinsky et al. [3]. In order to understand preponderance of spin-0 ground states with EGOE(2)-J, Zhao et al. [4] gave a simple procedure. Say there are $\mathscr{K}$ number of TBME. Then, put one of the TBME to -1, the rest to zero and calculate the spectrum. Repeat this procedure $\mathscr{K}$ times putting one of the TBME to -1 each time. Say K_J is number of times the ground state is found to have spin J. Then, the probability to find spin-0 ground states is $K_0/\mathscr{K}$. This prescription seem to work quite well as verified in many examples [4]. On the other hand, Zelevinsky et al. [3] invoked the idea of more attractive "geometric chaos". We will discuss this in Sect. 14.4 ahead. Papenbrock and Weidenmüller [6] used spectral radius R_J , the distance between lowest and highest state of levels with a given J, and its relation to spectral width σ_J. Numerical results showed that

$$R_J \sim r_J \sigma_J \tag{14.1}$$

with r_J approximately a constant independent of J. It is easy to see that for Gaussian density of eigenvalues, r_J will depend logarithmically on the matrix dimension. Distribution of σ_J discussed in Sect. 13.1.3 clearly show that spin-0 width will be relatively large compared to other J-widths (also with small fluctuations) and this gives preponderance of spin-0 ground states in shell model. In a recent investigation, Johnson [10] also emphasized the importance of spectral widths in understanding the preponderance of spin-0 ground states.

Kirson et al. [11] made an analysis of isospin structure of the ground states with random interactions. They have carried out nuclear shell model studies using EGOE$(1+2)$-JT in $(2s1d)$ space with 6 and 8 nucleons and varying $|N-Z|$. Figure 14.3 shows the main result of this work. It is clearly seen that random interactions distinguish between the ground state structure of even-even and odd-odd nuclei with the later having $J=1$ ground states more predominantly while it is $J=0$ for even-even nuclei. In addition, random interactions generate predominantly $T=T_{min}$ ground states and also natural isospin ordering.

14.3 Regularities in Ground State Structure in Two-Level Boson Systems: Mean-Field Theory

Large class of IBMs (see Figs. 14.4 and 14.5) admit two-level structure with degeneracy n_1 and n_2 respectively for the levels #1 and #2. One of the general group

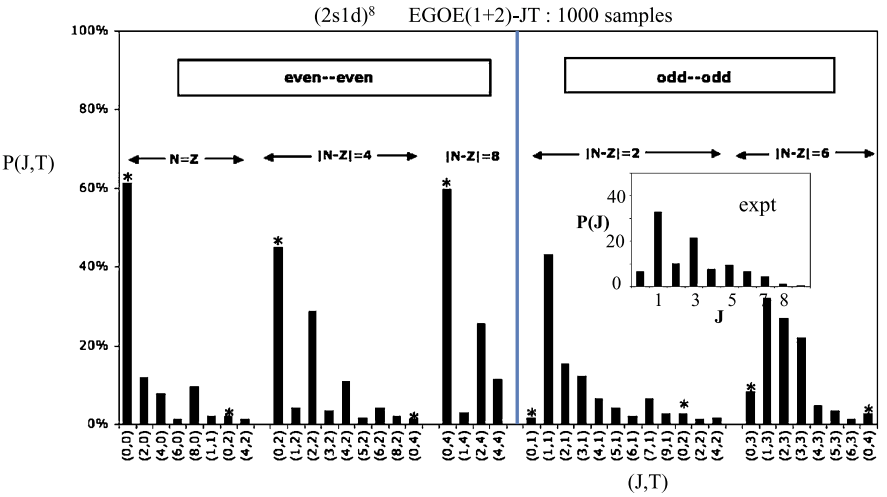

Fig. 14.3 Probability for ground states with (J, T) quantum numbers for $m = 6$ nucleons in $(2s1d)$ shell for a 9000 member EGOE(2)-JT. Note that in $(2s1d)$ shell there are 63 independent two-particle matrix elements. Results are shown for both even-even and odd-odd nuclei with $m = 6$. The $J = 0$ ground states are marked with a *asterisks*. Note that for odd-odd nuclei $J = 1$ ground states are more probable while for even-even nuclei (as expected) $J = 0$ ground states. Insect figure shows experimental data for the distribution of ground states with spin J for 276 odd-odd nuclei having positive parity ground states. Both the main figure and the insect figure are taken from [11] with permission from American Physical Society

structures generated by two-level models is $U(n) \supset G \supset SO(n_1) \oplus SO(n_2) \supset K$, $n_1 + n_2 = n$. Then, it is of interest to address the question of with what probability a given $SO(n_1) \oplus SO(n_2)$ irrep $[\omega_1] \oplus [\omega_2]$ will be the ground state in even-even nuclei with the Hamiltonians preserving $SO(n_1) \oplus SO(n_2)$ symmetry. There are two group-subgroup chains with this general structure. The group chains and the corresponding quantum numbers (irrep labels) for a m boson system for $n_1 \geq 3$ and $n_2 \geq 3$ situation are,

$$\begin{aligned}
&\text{(A):} \quad \left| \begin{array}{cccccc} U(n) & \supset & U(n_1) \oplus U(n_2) & \supset & SO(n_1) \oplus SO(n_2) & \supset K \\ \{m\} & & \{m_1\} \quad \{m_2\} & & [\omega_1] \quad [\omega_2] & \alpha \end{array} \right\rangle \\
&\qquad m_1 = 0, 1, 2, \ldots, m; m_2 = m - m_1 \\
&\qquad \omega_1 = m_1, m_1 - 2, \ldots, 0 \text{ or } 1, \omega_2 = m_2, m_2 - 2, \ldots, 0 \text{ or } 1 \qquad (14.2) \\
&\text{(B):} \quad \left| \begin{array}{ccccc} U(n) & \supset & SO(n) & \supset SO(n_1) \oplus SO(n_2) & \supset K \\ \{m\} & & [\omega] & [\omega_1] \quad [\omega_2] & \alpha \end{array} \right\rangle \\
&\qquad \omega = m, m - 2, \ldots, 0 \text{ or } 1, \omega_1 + \omega_2 = \omega, \omega - 2, \ldots, 0 \text{ or } 1.
\end{aligned}$$

Note that m_1 and m_2 denote number of bosons in levels #1 and # 2. Also, the algebra K in (14.2) is irrelevant for the discussion in this section. A general two-body Hamiltonian that mixes the states of these two chains but preserves the $[\omega_1]$ and $[\omega_2]$

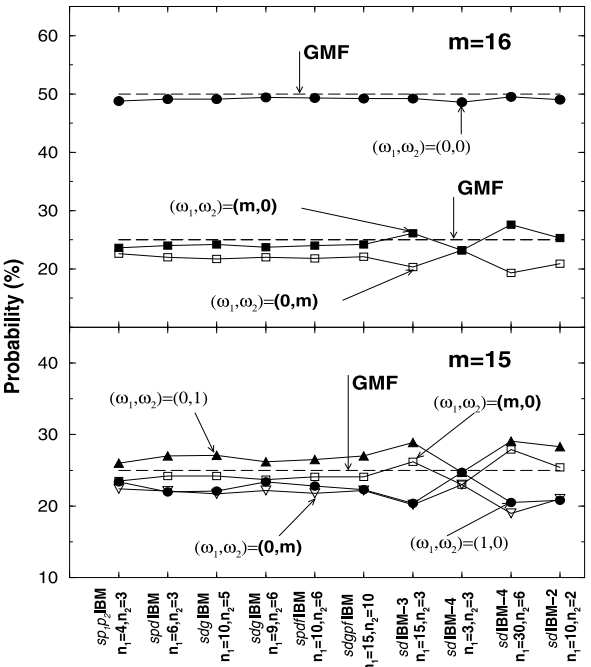

Fig. 14.4 Probabilities (in percentage) for $(\omega_1, \omega_2) = (0, 0)$, $(1, 0)$, (01), $(m, 0)$ and $(0, m)$ to be ground state irreps for various interacting boson models with $n_1 \geq 3$ and $n_2 \geq 2$. Note that for $pn - sd$IBM in the figure, $n_2 = 2$ and $(0, m) = (0, m) \oplus (0, -m)$. Calculations use 1000 members and the most general one plus two-body Hamiltonian interpolating the two symmetry limits. Figure is taken from [12] with permission from American Institute of Physics

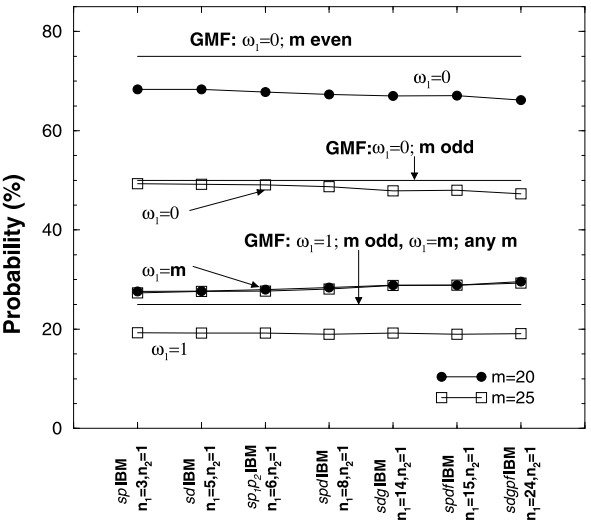

Fig. 14.5 Probabilities (in percentage) for $\omega_1 = 0$, 1 (only for odd m) and m to be ground state irreps for various interacting boson models with $n_1 \geq 3$ and $n_2 = 1$. Calculations use 1000 members and the most general one plus two-body Hamiltonian interpolating the two symmetry limits. Figure is taken from [12] with permission from American Institute of Physics

quantum numbers of $SO(n_1)$ and $SO(n_2)$ respectively [hereafter called $(\omega_1\omega_2)$] is,

$$\begin{aligned} H^{AB} &= \frac{1}{m}\big[\alpha_1 \mathscr{C}_1\big(U(n_1)\big) + \alpha_2 \mathscr{C}_1\big(U(n_2)\big)\big] \\ &\quad + \frac{1}{m(m-1)}\big[\alpha_3 \mathscr{C}_2\big(U(n_1)\big) + \alpha_4 \mathscr{C}_2\big(U(n_2)\big) + \alpha_5 \mathscr{C}_1\big(U(n_1)\big)\mathscr{C}_1\big(U(n_2)\big) \\ &\quad + \alpha_6 \mathscr{C}_2\big(SO(n)\big) + \alpha_7 \mathscr{C}_2\big(SO(n_1)\big) + \alpha_8 \mathscr{C}_2\big(SO(n_2)\big)\big]. \end{aligned} \tag{14.3}$$

Note that $\mathscr{C}_2(G)$ is the quadratic Casimir operator of G and $\mathscr{C}_1(U(r))$ is the number operator for the level r. In the basis (A), the α_6 term in Eq. (14.3) is the mixing part and all others are diagonal. Note that, in the situation $n_1 \geq 3$ and $n_2 = 1$, the $SO(n_2)$ algebra will not exist and hence $\mathscr{C}_2(SO(n_2))$ will not appear in Eq. (14.3). Then $(\omega_1\omega_2) \rightarrow (\omega_1)$ with $\omega_1 = 0, 1, 2, \ldots, \omega$ for chain (B). Similarly, for $n_1 \geq 3$ and $n_2 = 2$ one has $\omega_2 = \pm m_2, \pm(m_2 - 2), \ldots, \pm 1$ or 0 for chain (A) and $\omega_1 + |\omega_2| = \omega, \omega - 2, \ldots, 0$ or 1 for (B); thus, here $(\omega_1, \omega_2) \rightarrow (\omega_1, \pm\omega_2)$. Reference [13] gives more details. Starting with the basis defined by (A) and using the transformation brackets between (A) and (B) given in analytical form in [13], the matrix of H^{AB} can be constructed easily for a given m and $(\omega_1\omega_2)$. Calculations have been carried out for boson numbers $m =$ 10–25 for sdIBM [14], spIBM [15], spdIBM [16], sdgIBM [17], $sdpf$IBM [18], $sdgpf$IBM [19], sdIBM-2 [14], sdIBM-3 [20, 21] and sdIBM-4 [22] by choosing the parameters in Eq. (14.3) to be independent Gaussian variables with zero mean and variance unity. Some results obtained using 1000 samples of random interactions are given in Figs. 14.4 and 14.5.

A mean-field (MF) theory was developed in [8] for explaining the spIBM and sdIBM results. Its generalization explains the results for all IBMs [9]. In this generalized mean-field theory (GMF), intrinsic bosons y and z that correspond to the two levels are defined as $y_0^\dagger = \frac{1}{\sqrt{p}} \sum_{i=1}^{p} b_{\ell_i,0}^\dagger$ with $\sum_{i=1}^{p}(2\ell_i + 1) = n_1$ and $z_0^\dagger = \frac{1}{\sqrt{q}} \sum_{j=1}^{q} b_{\ell'_j,0}^\dagger$ with $\sum_{j=1}^{q}(2\ell'_j + 1) = n_2$. The angular momenta ℓ are real or fictitious. Then, the coherent state (CS) or the intrinsic state is

$$|m\alpha\rangle = \frac{1}{\sqrt{m!}}\big(\cos\alpha\, y_0^\dagger + \sin\alpha\, z_0^\dagger\big)^m |0\rangle \tag{14.4}$$

where α is a parameter with $-\pi/2 < \alpha \leq \pi/2$. Now, let us consider the simpler one parameter Hamiltonian [with only the α_2 and α_6 terms in Eq. (14.3)],

$$\begin{aligned} H &= \frac{1}{m}\cos\chi\,\hat{n}_2 + \frac{1}{m(m-1)}\sin\chi\, S_+ S_-, \\ S_+ &= S_+(1) - S_+(2) = \sum_{i=1}^{p} b_{\ell_i}^\dagger \cdot b_{\ell_i}^\dagger - \sum_{j=1}^{q} b_{\ell'_j}^\dagger \cdot b_{\ell'_j}^\dagger,\ S_- = (S_+)^\dagger. \end{aligned} \tag{14.5}$$

The range of χ is $-\pi/2 < \chi \leq 3\pi/2$. Now, the CS expectation value of H or the energy functional $E(\alpha)$ is,

$$E(\alpha) = \cos\chi \sin^2\alpha + \frac{1}{4}\sin\chi\cos^2 2\alpha. \tag{14.6}$$

The minimum of E divides (α, χ) into three ranges and they are: (i) $\alpha = 0$ for $-\pi/2 < \chi \leq \pi/4$; (ii) $\cos 2\alpha = \cot\chi$ for $\pi/4 \leq \chi \leq 3\pi/4$; (iii) $\alpha = \pi/2$ for $3\pi/4 < \chi \leq 3\pi/2$. Note that $\alpha = 0$ gives y-boson condensate with energy $E(\alpha = 0) \propto -\sin\chi\omega_1(\omega_1 + n_1 - 2)$. Then for even m, the ground state irreps are $(\omega_1\omega_2) = (00)$ with 25 % and $(\omega_1\omega_2) = (m0)$ with 12.5 % probability. Similarly $\alpha = \pi/2$ gives z-boson condensate with energy $E(\alpha = \pi/2) \propto -\sin\chi\omega_2(\omega_2 + n_2 - 2)$ and then the ground state irreps are $(\omega_1\omega_2) = (00)$ with 25 % and $(\omega_1\omega_2) = (0m)$ with 12.5 % probability. In the situation $\cos 2\alpha = \cot\chi$, cranking has to be done with respect to both $SO(n_1)$ and $SO(n_2)$. Evaluating moment of inertia, by an extension of the ordinary $SO(3)$ cranking, gives [9]

$$\begin{aligned} E &\propto \left[\frac{\omega_1(\omega_1 + n_1 - 2)}{A_+}\right] + \left[\frac{\omega_2(\omega_2 + n_2 - 2)}{A_-}\right]; \\ A_\pm &= \mp\frac{\sin\chi \pm \cos\chi}{\cos\chi\sin\chi}. \end{aligned} \tag{14.7}$$

This gives, $(m0)$ and $(0m)$ irreps to be ground states each with 12.5 % probability. Combining all the results will give for even m systems, $(\omega_1\omega_2) = (00)$, $(m0)$ and $(0m)$ irreps to be ground states with 50 %, 25 % and 25 % probability. For odd m, the y and z boson condensates give (10) and (01) irreps in place of (00) irrep. Therefore, for odd N systems, $(\omega_1\omega_2) = (10)$, (01), $(m0)$ and $(0m)$ irreps will be ground states with 25 % probability each. These GMF results for even and odd m are well verified in many examples for different IBMs as shown in Fig. 14.4. All these results are valid only for $n_1 \geq 3$ and $n_2 \geq 3$. However, these will also give the results for the situation with $n_1 \geq 3$ but $n_2 = 1$ with the following changes. With $n_2 = 1$, the irrep $[\omega_2]$ will not exist and then the irreps $(01) \rightarrow \omega_1 = 0$ and $(0m) \rightarrow \omega_1 = 0$. Therefore, for $n_1 \geq 3$ and $n_2 = 1$ the results are: (i) for even m, ground states will be $\omega_1 = 0$ and m with probability 75 % and 25 % respectively; (ii) for odd m, ground states will be $\omega_1 = 0$, 1 and m with probabilities 50 %, 25 % and 25 % respectively. These GMF results are well conformed in many numerical examples as shown in Fig. 14.5.

14.4 Regularities in Energy Centroids Defined over Group Irreps

Energy centroids defined over group irreps form simplest quantities for studying regularities generated by random interactions as it is possible to write simple formulas (exact in many situations and approximate in some) for these. Examples are

already given in the previous chapters. Energy centroids were first discussed by Mulhall et al. [23]. Later, Zhao et al. [24] analyzed fixed-L energy centroids in sdgIBM and also fixed-J energy centroids in shell model spaces using random interactions. Essentially here one is using EGOE$(1+2)$-J or EGOE$(1+2)$-JT in shell model and EGOE$(1+2)$-L in IBM's. They found that L_{min} (or J_{min}) and L_{max} (or J_{max}) will be lowest with largest probabilities and centroids with other L (or J) values are lowest with very small probability. Following these, in a number of examples, energy centroids with fixed spin or isospin, with fixed irreps of various group symmetries of both shell model and interacting boson models, in the presence of random two-body and three-body interactions have been studied by recognizing that simple propagation formulas can be written for energy centroids in many situations [25–29]. The examples studied are:

1. $U_{sd}(6) \supset SU_{sd}(3)$ energy centroids $\overline{E_{m,(\lambda\mu)}}$ in sdIBM with two- and three-body interactions; $(\lambda\mu)$ are $SU(3)$ irreps,
2. $\overline{E_{(m_1\omega_1,m_2\omega_2,\ldots)}}$ of $U(\mathcal{N}) \supset \sum_i [U(\mathcal{N}_i) \supset SO(\mathcal{N}_i)] \oplus$ in IBM's [$m = \sum_i m_i$ and ω_i are the irreps of $SO(\mathcal{N}_i)$] with the specific example of sdgIBM,
3. $\overline{E_{m,(\lambda\mu),T}}$ of $U(3\mathcal{N}) \supset U(\mathcal{N}) \otimes [SU_T(3) \supset O_T(3)]$ in IBM-T [i.e. IBM with bosons carrying isospin $T = 1$ degree of freedom and this is also called IBM-3] with the specific example of sdIBM-T with both two- and three-body interactions,
4. $\overline{E_{m,\{f\},[\sigma]}}$ of $U(6\mathcal{N}) \supset U(\mathcal{N}) \otimes [SU_{ST}(6) \supset O_{ST}(6)]$ in IBM-ST [i.e. IBM with the bosons carrying spin-isospin degrees of freedom $(ST) = (10) \oplus (01)$ and this is also called IBM-4] with the specific example of sdIBM-ST,
5. $\overline{E_{n_{sd}(\lambda_{sd}\mu_{sd}):n_{pf}(\lambda_{pf}\mu_{pf})}}$ of $U_{sdpf}(16) \supset [U_{sd}(6) \supset SU_{sd}(3)] \oplus [U_{pf}(10) \supset SU_{pf}(3)]$ in $sdpf$IBM,
6. $\overline{E_{m,\omega}}$ in $U(\mathcal{N}) \supset SO(\mathcal{N})$ of IBMs; $[\omega]$ are irreps of $SO(\mathcal{N})$,
7. $\overline{E_{\{f\}(ST)}}$ of $U(24) \supset U(6) \otimes [SU_{\{f\}}(4) \supset SU_S(2) \otimes SU_T(2)]$ in shell model for $(2s1d)$ shell nuclei,
8. $\overline{E_{m,T}}$ of $U(2\mathcal{N}) \supset U(\mathcal{N}) \otimes SU_T(2)$ in shell model spaces with two- and three-body interactions,
9. $\overline{E_{m,\{f\},(\lambda\mu)}}$ of $U(24) \supset [U(6) \supset SU(3)] \otimes SU_{\{f\}}(4)$ for $(2s1d)$ shell nuclei,
10. $\overline{E_{m,J}}$ for $(j)^m$ system of fermions and $\overline{E_{m,L}}$ for $(\ell)^m$ system of boson with two- and three-body interactions (here approximate formulas given in Sect. 13.1.2 are used).

In all these examples it is seen that, with random interactions, the energy centroids over highest and lowest irreps are lowest in energy with large ($\gtrsim$90 %) probability. For illustration, let us consider the example of $\overline{E_{m,\omega}}$ where $[\omega]$ are irreps of $SO(\mathcal{N})$ in $U(\mathcal{N}) \supset SO(\mathcal{N})$ of IBM's; $\mathcal{N} = 6$ for sdIBM, 15 for sdgIBM and 16 for $sdpf$IBM. With $\omega = m, m-2, \ldots, 0$ or 1 and the matrix elements of boson pairing operator H_P being $\frac{1}{4}(m-\omega)(m+\omega+\mathcal{N}-2)$, we have, $\overline{E_{m,\omega}} = E_0(m) + [(m-\omega)(m+\omega+\mathcal{N}-2)/2\mathcal{N}][\overline{E_{2,0}} - \overline{E_{2,2}}]$. Then clearly energy centroids with highest and lowest ω will be lowest in energy with 50 % probability each. In another example, consider fixed isospin centroids $\overline{E_{(m,T)}}$ generated

by a 3-body Hamiltonian. It is easily seen that, $\overline{E_{(m,T)}} = \{\frac{m^3-6m^2+8}{12} - \frac{2T(T+1)}{3} + \frac{mT(T+1)}{3}\}\overline{E_{3,\frac{3}{2}}} + \{\frac{m^3-4m}{12} + \frac{2T(T+1)}{3} - \frac{mT(T+1)}{3}\}\overline{E_{3,\frac{1}{2}}}$ and this implies

$$\overline{E_{(m,T_{max})}} - \overline{E_{(m,T)}} = \{\overline{E_{3,\frac{3}{2}}} - \overline{E_{3,\frac{1}{2}}}\}\left(\frac{m-2}{3}\right)\{T_{max}(T_{max}+1) - T(T+1)\}. \tag{14.8}$$

Equation (14.8) shows that for m nucleons, even with random 3-body Hamiltonians, just as with 2-body Hamiltonians, $T = T_{max}$ and $T = 0$ energy centroids will be lowest in energy each with 50 % probability. Now we will discuss some select non trivial examples.

14.4.1 sdgIBM Energy Centroids

Spectrum generating algebra for sdgIBM is $U(15)$ and one of the decompositions of the m boson space is according to $(m_s, m_d, v_d, m_g, v_g)$ where m_s, m_d and m_g are s, d and g boson numbers with the total boson number $m = m_s + m_d + m_g$. Similarly v_d and v_g are the d and g boson seniority quantum numbers, $v_d = m_d, m_d - 2, \ldots, 0$ or 1 and $v_g = m_g, m_g - 2, \ldots, 0$ or 1. Then, it is possible to consider regularities in fixed-$(m_s, m_d, v_d, m_g, v_g)$ energy centroids using the propagation formula [26],

$$\begin{aligned}
\overline{E_{(m_s,m_d,v_d,m_g,v_g)}} &= \sum_i m_i\varepsilon_i + \sum_{i>j}\overline{V_{ij}}m_i m_j + \sum_i \frac{m_i(m_i-1)}{2}\langle V\rangle^{m_i'=2,\omega_i=2} \\
&\quad + \sum_i \frac{\langle V\rangle^{m_i'=2,\omega_i=0} - \langle V\rangle^{m_i'=2,\omega_i=2}}{2\mathcal{N}_i}(m_i - v_i) \\
&\quad \times (m_i + v_i + \mathcal{N}_i - 2); \\
\overline{V_{ij}} &= \left\{\left[\mathcal{N}_i(\mathcal{N}_j + \delta_{ij})\right]/(1+\delta_{ij})\right\}^{-1}\sum_L V^L_{\ell_i\ell_j\ell_i\ell_j}(2L+1), \\
\langle V\rangle^{m_i'=2,\omega_i=0} &= \left\langle(\ell_i\ell_i)L_i = 0\middle|V\middle|(\ell_i\ell_i)L_i = 0\right\rangle, \\
\langle V\rangle^{m_i'=2,\omega_i=2} &= \left[\frac{\mathcal{N}_i(\mathcal{N}_i+1)}{2} - 1\right]^{-1}\left[\frac{\mathcal{N}_i(\mathcal{N}_i+1)}{2}\overline{V_{ii}} - \langle V\rangle^{m_i=2,\omega_i=0}\right].
\end{aligned} \tag{14.9}$$

Here, $i = s$, d and g and $\mathcal{N}_s = 1$, $\mathcal{N}_d = 5$ and $\mathcal{N}_g = 9$. Also, for two particles, m_i is denoted by m_i' and v_s, v_d and v_g are denoted by ω_s, ω_d and ω_g respectively. Similarly, ε_i are the 3 sp energies $(\varepsilon_s, \varepsilon_d, \varepsilon_g)$ and $V^L(\ell_1, \ell_2, \ell_1, \ell_2)$ the 16 diagonal two-particle matrix elements. For the s orbit, $m_s = 2$ and $\omega_s = 2$ and there will be no two-boson state with $\omega_s = 0$. Therefore, the fourth term in the centroid formula is only for $i = d$ and g. Note that for m_s bosons, trivially $v_s = m_s$ and hence it is not specified. The 19 parameters (3 sp energies and 16 TBME) in sdgIBM are chosen to be Gaussian random variables with zero center and unit variance. To maintain proper scaling, the sp energies are divided by m and the two

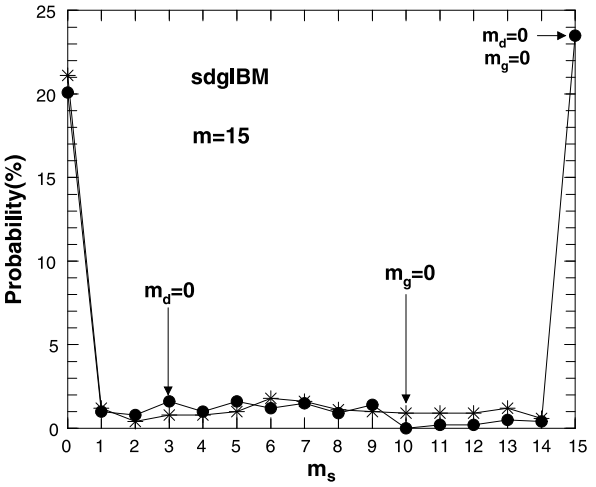

Fig. 14.6 Probabilities for sdgIBM fixed-$(m_s, m_d, v_d, m_g, v_g)$ energy centroids to be lowest in energy vs m_s for a system of 15 bosons ($m = 15$). For each m_s, the probability shown is the sum of the probabilities for the irreps with the seniority quantum number lowest ($v_\ell = v_\ell^{min}$) and highest ($v_\ell = m_\ell$). *Filled circles* and *stars* are for configurations with $m_d = 0$ and $m_g = 0$ respectively; they are joined by *lines* to guide the eye. Figure is taken from [26] with permission from American Physical Society

particle matrix elements by $m(m-1)$. Numerical results obtained for a 1000 member ensemble with $m = 15$ are given in Fig. 14.6. Let us denote $v_d = 0$ or 1 (for m_d is even or odd respectively) by v_d^{min} and similarly v_g^{min} is defined. As seen from the figure, configurations $(m_s, m_d = v_d = m - m_s, m_g = v_g = 0)$, $(m_s, m_d = m - m_s, v_d = v_d^{min}, m_g = v_g = 0)$, $(m_s, m_d = v_d = 0, m_g = v_g = m - m_s)$ and $(m_s, m_d = v_d = 0, m_g = m - m_s, v_g = v_g^{min})$ exhaust about 91 % probability. In this, the configurations with $m_s = m_d = 0$ carry ∼20 %, $m_s = m_g = 0$ carry ∼21 % and $m_s = m$ carry ∼24 % probability. Thus the configurations with $m_s = 0, m$ are most probable but others give non negligible probability for being the lowest.

14.4.2 sdIBM-T Energy Centroids with 3-Body Forces

In the second example we will consider $\overline{E_{m,(\lambda\mu),T}}$ of $U_{sd}(18) \supset U(6) \otimes [SU_T(3) \supset SO_T(3)]$ in sdIBM-3 with three body interactions. Firstly the $U_{sd}(18)$ irrep is the totally symmetric irrep $\{m\}$ and the $SU_T(3)$ irreps [same as those of $U(6)$] are $(\lambda, \mu) = ((f_1 - f_2), (f_2 - f_3))$ where $f_1 + f_2 + f_3 = m$ and $f_1 \geq f_2 \geq f_3 \geq 0$. The $(\lambda\mu) \rightarrow T$ reductions follow from Elliott's rules [30] given by Eq. (10.32). Counting of number of irreps $(\lambda\mu)T$ for $m \leq 3$ shows that besides the operators 1, $\hat{n}$, $\hat{C}_2$, $\hat{C}_3$ and $\hat{T}^2$, we need one extra $SO_T(3)$ scalar in $SU_T(3)$. The well known $SU(3) \supset SO(3)$ integrity basis operator $\hat{X}_3$ defined by Eq. (10.36), which is three-

body, is useful here. Fixed-$(\lambda\mu)T$ averages of the $\hat{X}_3$ operator are given by [31]

$$X_3\big((\lambda\mu)T\big) = \langle \hat{X}_3 \rangle^{(\lambda\mu)T} = (-1)^{1-\delta_{\mu,0}} \frac{[3-4T(T+1)]\sqrt{T(T+1)}}{\sqrt{(2T-1)(2T+3)}} \times \sqrt{C_2(\lambda\mu)} \frac{\sum_k \langle (\lambda\mu) k T(11) 2 \,||\, (\lambda\mu) k T \rangle_{\rho=1}}{\sum_{k'} 1}. \tag{14.10}$$

In Eq. (14.10), $\langle --- \,||\, --- \rangle$ are $SU_T(3) \supset SO_T(3)$ reduced Wigner coefficients and these coefficients can be calculated, as stated in Chap. 10, using the programs in [32]. Using $\hat{X}_3$ averages for $m \leq 3$, propagation formula for $\overline{E_{m,(\lambda\mu),T}}$ has been derived in [29] and the result is [with $T^2 = T(T+1)$ and $X_3((\lambda\mu)T) = \langle \hat{X}_3 \rangle^{(\lambda\mu)T}$],

$$\begin{aligned}
&\overline{E_{m,(\lambda\mu),T}} \\
&= \left[\frac{7m}{9} - \frac{7m^2}{18} - \frac{7C_2(\lambda\mu)}{90} - \frac{7T^2}{30} + \frac{7m^3}{162} + \frac{7mC_2(\lambda\mu)}{270} + \frac{7mT^2}{90} \right. \\
&\quad \left. - \frac{C_3(\lambda\mu)}{90} + \frac{X_3((\lambda\mu)T)}{45}\right] \overline{E_{3,(30),3}} \\
&\quad + \left[\frac{m}{3} - \frac{m^2}{6} - \frac{C_2(\lambda\mu)}{5} + \frac{7T^2}{30} + \frac{m^3}{54} + \frac{mC_2(\lambda\mu)}{15} - \frac{7mT^2}{90} + \frac{C_3(\lambda\mu)}{15} \right. \\
&\quad \left. - \frac{X_3((\lambda\mu)T)}{45}\right] \overline{E_{3,(30),1}} \\
&\quad + \left[-\frac{m}{3} + \frac{C_2(\lambda\mu)}{6} - \frac{T^2}{12} + \frac{m^3}{27} - \frac{mT^2}{18} - \frac{C_3(\lambda\mu)}{6} + \frac{X_3((\lambda\mu)T)}{18}\right] \overline{E_{3,(11),1}} \\
&\quad + \left[-\frac{5m}{9} + \frac{C_2(\lambda\mu)}{6} + \frac{T^2}{12} + \frac{5m^3}{81} - \frac{2mC_2(\lambda\mu)}{27} + \frac{mT^2}{18} + \frac{C_3(\lambda\mu)}{18} \right. \\
&\quad \left. - \frac{X_3((\lambda\mu)T)}{18}\right] \overline{E_{3,(11),2}} \\
&\quad + \left[\frac{m}{9} + \frac{m^2}{18} - \frac{C_2(\lambda\mu)}{18} + \frac{m^3}{162} - \frac{mC_2(\lambda\mu)}{54} + \frac{C_3(\lambda\mu)}{18}\right] \overline{E_{3,(00),0}}.
\end{aligned} \tag{14.11}$$

Using Eq. (14.11) calculations have been carried out in [29] for boson numbers $m = 10 - 20$ bosons using a 1000 member random 3-body ensemble obtained by treating $\overline{E_{3,(\lambda\mu),T}}$ as Gaussian random variables with zero center and unit variance and the results are shown in Fig. 14.7. Energy centroids of highest [according to $C_2(\lambda\mu)$ value] $(\lambda\mu)$ with lowest and highest T values and the lowest $(\lambda\mu)$ carry $\sim$88 % probability for being lowest in energy. The only other irrep that carries significant probability ($\sim$9 %) is $(0, \frac{m}{2})T = 0$ for m even and $(1, \frac{m-1}{2})T = 1$ for m odd. Thus, random 3-body interactions generate regularities in energy centroids.

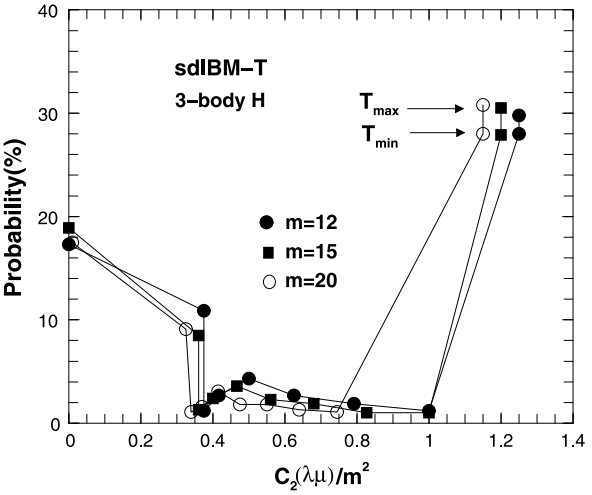

Fig. 14.7 Probabilities for the sdIBM-T energy centroids $\overline{E_{m,(\lambda\mu),T}}$ to be lowest in energy vs $C_2(\lambda\mu)/m^2$ for boson systems with $m = 12$, 15 and 20. For the highest $(\lambda\mu)$, the probabilities for both highest and lowest T are shown and for the lowest $(\lambda\mu)$ only one T value is possible. For the irreps not shown in the figure, the probability is less than 0.1 %. All the points for a given m are joined by *lines* to guide the eye. Figure is taken from [29] with permission from World Scientific

14.4.3 SU(4)-ST Energy Centroids

For $(2s1d)$ shell nuclei, $U(24)$ is the spectrum generating algebra and the spin-isospin (ST) supermultiplet $SU(4)$ algebra appears in the subalgebra $U(24) \supset U(6) \otimes \{SU(4) \supset SU_S(2) \otimes SU_T(2)\}$; note that $U(6)$ generates the orbital part. For a given number of nucleons m, the allowed $U(4)$ irreps are $\{f\} = \{f_1, f_2, f_3, f_4\}$ with $f_1 \geq f_2 \geq f_3 \geq f_4 \geq 0$, $f_1 \leq 6$ and $f_1 + f_2 + f_3 + f_4 = m$ and the $U(6)$ irreps, by direct product nature, are $\{\tilde{f}\}$, the transpose of $\{f\}$. It is important to note that the equivalent $SU(4)$ irreps are $\{f_1 - f_4, f_2 - f_4, f_3 - f_4\}$. With these, from now on we will use $U(4)$ and the irreps $\{f\}$. It is well known that a totally symmetric $U(4)$ irrep $\{\lambda\} \rightarrow (ST) = (\frac{\lambda}{2}, \frac{\lambda}{2}), (\frac{\lambda}{2} - 1, \frac{\lambda}{2} - 1), \ldots, (00)$ or $(\frac{1}{2}, \frac{1}{2})$. Using this result and expanding a given $U(4)$ irrep into totally symmetric $U(4)$ irreps will give easily $\{f\} \rightarrow (ST)$ reductions. Just as the fixed-T energy centroids propagate, the fixed $\{f\}(ST)$ energy centroids $\overline{E_{\{f\}(ST)}}$ for a one plus two-body Hamiltonian propagate as the available scalars of maximum body rank 2 are $1, \hat{n}, \hat{n}^2, C_2(U(4)), S^2$ and T^2 and the centroids for $m \leq 2$ are also six in number. The propagation equation, with $C_2(\{f\}) = \sum_i f_i^2 + 3f_1 + f_2 - f_3 - 3f_4$ where $C_2(\{f\})$ gives the eigenvalues of the quadratic Casimir invariant of $U(4)$, is [33]

$$\begin{aligned}\overline{E_{\{f\}(ST)}} = {} & \big(1 - 3m + m^2\big)\langle H\rangle^{\{0\}(00)} + \big(2m - m^2\big)\langle H\rangle^{\{1\}(\frac{1}{2}\frac{1}{2})} \\ & + \left[-\frac{9}{8}m + \frac{1}{4}m^2 + \frac{1}{8}C_2\big(\{f\}\big) + \frac{1}{4}S(S+1) + \frac{1}{4}T(T+1)\right]\langle H\rangle^{\{2\}(11)} \\ & + \left[-\frac{1}{8}m + \frac{1}{8}C_2\big(\{f\}\big) - \frac{1}{4}S(S+1) - \frac{1}{4}T(T+1)\right]\langle H\rangle^{\{2\}(00)}\end{aligned}$$

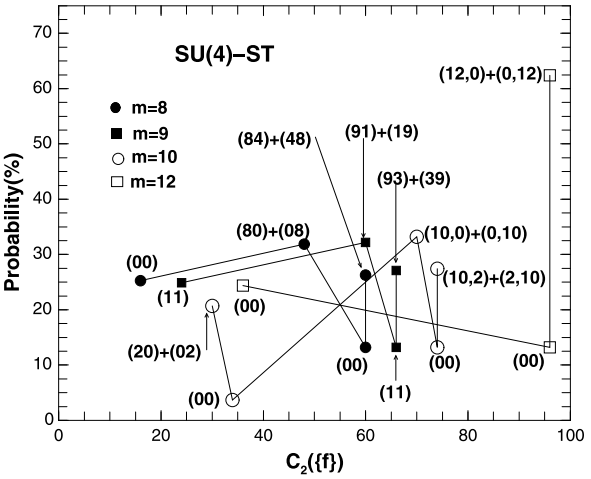

Fig. 14.8 Probabilities for the $(2s1d)$ shell energy centroids $\overline{E_{\{f\}(ST)}}$ to be lowest in energy vs $C_2(\{f\})$. Results are shown for nucleon numbers $m = 8$, 9, 10 and 12. The $U(4)$ irreps $\{f\}$ for the results in the figure are given in the text. The corresponding (ST) values are shown in the figure. All the *points* for a given m are joined by *lines* to guide the eye. Figure is taken from [28] with permission from American Physical Society

$$+\left[\frac{3}{8}m+\frac{1}{8}m^2-\frac{1}{8}C_2\big(\{f\}\big)+\frac{1}{4}S(S+1)-\frac{1}{4}T(T+1)\right]\langle H\rangle^{\{1^2\}(10)}$$
$$+\left[\frac{3}{8}m+\frac{1}{8}m^2-\frac{1}{8}C_2\big(\{f\}\big)-\frac{1}{4}S(S+1)+\frac{1}{4}T(T+1)\right]\langle H\rangle^{\{1^2\}(01)}. \tag{14.12}$$

Considering the basic energy centroids $\langle H\rangle^{\{f\}(ST)}$ with $m \leq 2$ as independent zero centered (with unit variance) Gaussian random variables, instead of using ε_i and $V_{ijkl}^{J,t=0.1}$ as random variables, the $\{f\}(ST)$ structure of the ground states has been studied in [28]. Figure 14.8 shows results obtained using 1000 samples for $m = 8$–12. The probabilities split into three $U(4)$ irreps (other irreps carry less than 1 % probability and they are not shown in the figure) for $n = 8$, 9 and 10 and the corresponding (ST) values are as shown in the figure. Energy centroids with the lowest and highest $U(4)$ irreps carry ∼25 % and ∼40 % respectively. The lowest irreps are $\{2^4\}$, $\{32^3\}$ and $\{3^22^2\}$ for $n = 8$, 9 and 10 respectively and the highest irreps are $\{6, n-6\}$. The third irreps $\{4^2\}$, $\{54\}$ and $\{5^2\}$, with probability ∼32 %, for $n = 8$, 9 and 10 respectively are those that carry $S = n/2$ or $T = n/2$; for $n = 10$ the irrep $[3^31](00)$ carries 3.7 % probability. For the mid-shell example with $n = 12$, the probabilities split into the lowest $\{3^4\}$ and highest $\{6^2\}$ irreps with ∼25 % and ∼75 % respectively. The lowest irrep supports only $(ST) = (00)$ and the probability for the highest irrep splits into ∼13 % and ∼62 % for $(ST) = (00)$ and $(12, 0) + (0, 12)$. Figure also shows that the probability for the energy centroid with lowest $U(4)$ irrep to be lowest is only ∼25 % and it should be noted that the corresponding $SU(4)$ irreps are $\{0\}(00)$, $\{1\}(\frac{1}{2}\frac{1}{2})$ and $\{1^2\}(10) + (01)$ respectively for $n = 4k$, $4k + 1$ and $4k + 2$ with k being a positive integer. This result is in agreement with EGOE$(1 + 2)$-JT calculations carried out using nuclear shell model codes in [34].

14.4.4 $(j)^m$ and $(\ell)^m$ Systems with 2- and 3-Body Interactions: Geometric Chaos

In the final example we will consider spin J centroids $\overline{E_{(m,J)}}$ generated by random 2-body and 3-body Hamiltonians for m identical fermions in a single j shell, i.e. EGOE(2)-$(j:J)$ and EGOE(3)-$(j:J)$ energy centroids. The $\overline{E_{(m,J)}}$'s correspond to averages of H over the space defined by the irreps m and J of $U(2j+1)$ and $SO(3)$ respectively in $U(2j+1) \supset SO(3)$. As discussed in Sect. 13.1.2, $\overline{E_{(m,J)}}$ can be expanded in powers of $J(J+1)$ and to a good approximation one can truncate the expansion to $[J(J+1)]^2$ term. Then, for a 2-body H, the probability P_0 for $\overline{E_{(m,J=0)}}$ to be lowest in energy is given by Eq. (13.20). Application of this shows that P_0 is close to 50 %. This result is in direct correlation with the numerically observed result (see Table 14.1) that the probability for $J=0$ ground states is ~50 % with random 2-body interactions. To the extent that only lower order moments of the eigenvalue density $\rho(E)$ determine the ground states, one can argue that the regularities of the energy centroids and spectral variances (see next section) result in regularities in $J=0$ ground states. The energy centroids and spectral variances average out many J-couplings in m particle spaces—a geometric effect—giving propagation equations (exact or approximate). Thus, it is possible to argue that the preponderance of $J=0$ ground states (similarly other regularities) generated by random interactions is a geometric effect and in [23] this is termed *geometric chaos*. It should be added that a precise definition of *geometric chaos* is still lacking. It is good to recall here that for EE, in addition to a classical ensemble in the defining space (2-particle space for two-body interactions), there is information propagation from the defining space to m particle spaces. This geometric aspect is absent in classical ensembles.

Turning to 3-body H, Eq. (13.12) gives the formula for $\overline{E_{(m,J)}}$ to order $J(J+1)$ to be,

$$\overline{E_{(m,J)}} = \left[\langle H(3)\rangle^m - \frac{3}{2}\frac{\langle J_z^2 \widetilde{H(3)}\rangle^m}{\langle J_z^2\rangle^m}\right] + \frac{1}{2}\frac{\langle J_z^2 \widetilde{H(3)}\rangle^m}{[\langle J_z^2\rangle^m]^2} J(J+1) \tag{14.13}$$

and this is good for $m \gg 3$, $j \gg m$ and j large. In Eq. (14.13), $\widetilde{H}$ is H with the average part $\langle H\rangle^m$ removed. Denoting three particle antisymmetric states by $|(j)^3;\alpha J_3\rangle$ with α being the extra label required to completely specify the states, diagonal 3-particle matrix elements of $H(3)$ are $G_{\alpha J_3} = \langle (j)^3;\alpha J_3 \mid H(3) \mid (j)^3;\alpha J_3\rangle$. It is easy to see that,

$$\begin{aligned} \langle H(3)\rangle^m &= \binom{m}{3}\langle H(3)\rangle^3 = \binom{m}{3}\binom{2j+1}{3}^{-1}\sum_{\alpha,J_3} G_{\alpha J_3}(2J_3+1), \\ \langle J_z^2\rangle^m &= \frac{1}{3}\langle J^2\rangle^m = \frac{1}{6}m(2j+1-m)(j+1) \simeq \frac{m}{3}j(j+1). \end{aligned} \tag{14.14}$$

Tensorial decomposition of J^2 and H operators with respect to $U(2j+1)$ will give $J^2 = (J^2)^{\nu=0} + (J^2)^{\nu=2}$ and $H(3) = H^{\nu=0}(3) + H^{\nu=2}(3) + H^{\nu=3}(3)$.

Single most important property of this decomposition is that it is orthogonal with respect to m particle averages. Then, $\widetilde{H} = H - H^{\nu=0}$ gives $\langle J^2 \widetilde{H(3)} \rangle^m = \langle (J^2)^{\nu=2} H^{\nu=2}(3) \rangle^m = \langle (J^2)^{\nu=2} H(3) \rangle^m$. Also, Eq. (4.18) gives $H^{\nu=2}(3) = (\hat{n} - 2) F^{\nu=2}(2)$ where F is a two-body operator with rank $\nu = 2$ and $\hat{n}$ is number operator. These will give $\langle (J^2)^{\nu=2} H(3) \rangle^m = \frac{m(m-1)(m-2)(2j+1-m)(2j-m)}{6(2j-2)(2j-3)} \times \langle (J^2)^{\nu=2} H(3) \rangle^3$. Now the final formula for $\overline{E_{(m,J)}}$ is [28],

$$\overline{E_{(m,J)}} \simeq E_0 + \frac{3m}{2} \left[\frac{\sum_{\alpha, J_3} \{J_3(J_3+1) - 3j(j+1)\} G_{\alpha J_3} (2J_3+1)}{[j(j+1)(2j+1)]^2 (2j+1)} \right] J(J+1). \tag{14.15}$$

Thus, the $J(J+1)$ term will have linear m dependence. An interesting observation in many numerical calculations (not only with single j but also multi-j and JT centroids) is $\langle \overline{E_{(m,J)}} \rangle_{min} \sim E_0 + C J(J+1)$ where $\langle \overline{E_{(m,J)}} \rangle_{min}$ is the average of $\overline{E_{(m,J)}}$ over the members of the EGOE(3)-$(j : J)$ ensemble for which $\overline{E_{(m,J)}}$ with $J \sim J_{min}$ is lowest in energy. The coefficient C follows from Eq. (14.15) and it is given by

$$C = \sqrt{\frac{2}{\pi}} \sqrt{\sum_{\alpha, J_3} \left[\left\{ J_3(J_3+1) - 3j(j+1) \right\} (2J_3+1) \right]^2} \times \frac{3m}{2[j(j+1)(2j+1)]^2 (2j+1)}. \tag{14.16}$$

For two-body interactions, i.e. for EGOE(2)-$(j : J)$, C will be independent of m and this follows from Eq. (13.15). Thus 3-body H's give m dependence to C that is absent for a two-body H. Finally, Eq. (14.15) extends easily to $(\ell)^m$ boson systems giving [28],

$$\overline{E_{(m,L)}} \simeq E_0 + 6m \left[\frac{\sum_{\alpha, L_3} \{L_3(L_3+1) - 3\ell(\ell+2)\} G_{\alpha L_3} (2L_3+1)}{[\ell^2 (2\ell+1)(2\ell+2)(2\ell+3)(2\ell+4)(2\ell+5)]} \right] L(L+1) \tag{14.17}$$

where $G_{\alpha L_3}$ are three-body matrix elements for bosons with spin L_3. This gives $C \sim 0.033m$ for d boson systems and compares well with the numerical calculations with a 1000 member BEGOE(3)-$(\ell = 2 : L)$ that gave $0.035m$ as reported in [28].

Going beyond 2- and 3-body ensembles, Volya [35] has analyzed EGOE(k)-$(j : J)$ ensembles for $(j)^m$ systems, with $k < m$, and argued using the numerical results that symmetries emerge out of random interactions. This and the related argument [36] that symmetries are responsible for chaos or random matrix behavior in nuclear shell model certainly deserve much further study.

14.5 Regularities in Spectral Variances over Group Irreps with Random Interactions

Going beyond energy centroids, many different types of correlations involving spectral variances can be studied in order to understand the origin of regular structures generated by random interactions. Some studies of spectral variances defined over good symmetry subspaces, i.e. fixed-m variances for EGOE(k)/EGUE(k), fixed-(m, S) variances for EGOE(2)-**s** and fixed-(m, J) variances for EGOE(2)-J are already discussed in Chaps. 4, 6 and 9–13. In addition, variances $\sigma^2(\Gamma)$ over subspaces (Γ) defined over broken symmetries of nuclear shell model and the interacting boson models (similarly for other finite quantum systems) yield valuable information. Here Γ are the irreps of G in $U(N) \supset G \supset G_f$ with G_f being a symmetry of H such as $SO_J(3)$ and G is a broken symmetry such as the configuration symmetry in nuclear shell model. Important point here being that the variances $\sigma^2(\Gamma) = \langle (H - \langle H \rangle^\Gamma)^2 \rangle^\Gamma$ determine much of the statistical behavior of strength functions or partial densities $\langle \delta(H - E) \rangle^\Gamma$. Here, we will present results for $\overline{\sigma^2(\Gamma)}$ for some EGOEs. Firstly it is important to note that $\sigma^2(\Gamma)$, just as energy centroids, propagate in a simple manner in many situations. For example, for shell model spherical configurations $(\mathbf{m}) = (m_1, m_2, \ldots)$ where m_i is number of particles in the shell model j_i orbit and similarly for interacting boson models (with or without internal degrees of freedom), the configuration variances $\sigma^2(\mathbf{m})$ are given by,

$$\sigma^2(\mathbf{m}) = \sum_{i \geq j, k \geq \ell} \frac{m_i(m_j - \delta_{ij})(N_k \mp m_k)(N_\ell \mp m_\ell \mp \delta_{k\ell})}{N_i(N_j \mp \delta_{ij})(N_k \mp \delta_{ki} \mp \delta_{kj})(N_\ell \mp \delta_{\ell i} \mp \delta_{\ell j} \mp \delta_{\ell k})} \times \sum_\Gamma \left(\tilde{V}^\Gamma_{ijkl}\right)^2 [\Gamma]. \tag{14.18}$$

In Eq. (14.18), N_i is the degeneracy of the i-th orbit, Γ is two-particle J or JT in shell model and L (or LT or LST) in IBMs. Similarly, $[\Gamma]$ is the dimension of the Γ space and for example, $[J] = (2J + 1)$ and $[JT] = (2J + 1)(2T + 1)$. With $\overline{V}_{ij}$ the average two-particle matrix element for particles in the orbits i and j, we have $\tilde{V}^\Gamma_{ijij} = V^\Gamma_{ijij} - \overline{V}_{ij}$ and for the rest $\tilde{V}^\Gamma_{ijkl} = V^\Gamma_{ijkl}$. Finally in $\mp$ in Eq. (14.18), the upper sign is for fermions (shell model) and the lower sign is for bosons (IBMs).

Some of the other situations where it is possible to write propagation equations are [37, 38]:

1. $U_{sd}(6) \supset SU_{sd}(3)$ variances $\sigma^2(m, (\lambda\mu))$ in sdIBM,
2. $\sigma^2(m, [\omega])$ of $U(\mathscr{N}) \supset SO(\mathscr{N})$ in sdIBM, sdgIBM, sdIBM-T, $sdpf$IBM etc. [$[\omega]$ are irreps of $SO(\mathscr{N})$],
3. $\sigma^2(\mathbf{m}, \boldsymbol{\omega}) = \sigma^2(m_1, \omega_1; m_2, \omega_2; \ldots)$ of $U(\mathscr{N}) \supset \sum_i [U(\mathscr{N}_i) \supset SO(\mathscr{N}_i)] \oplus$ in IBMs [ω_i are the irreps of $SO(\mathscr{N}_i)$] and similarly in shell model with $SO(\mathscr{N}_i)$ replaced by $Sp(\mathscr{N}_i)$. The $\sigma^2(\mathbf{m})$ in Eq. (14.18) corresponds to $U(\mathscr{N}) \supset \sum_i U(\mathscr{N}_i) \oplus$,

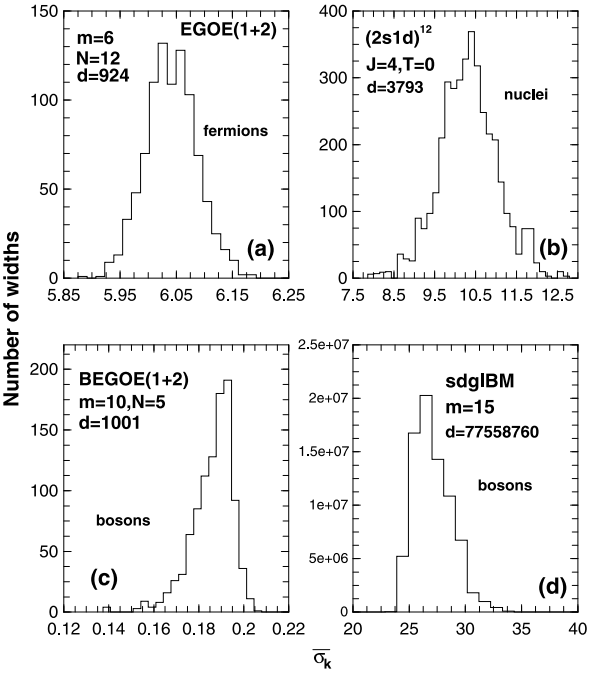

Fig. 14.9 Distribution of ensemble averaged (except in (**b**)) widths over the irreps k in 4 examples. In the histograms, at the center of each bin, the number of widths in the corresponding bin gives the height of the bin. Adding the number of widths will give the matrix dimension d. Values of d are given in the figures. Results are shown for: (**a**) EGOE$(1+2)$ for spinless fermions; (**b**) a $(2s1d)$ nuclear shell model example; (**c**) BEGOE$(1+2)$ for spinless bosons; (**d**) BEGOE$(1+2)$-L for sdgIBM. In (**b**), the widths are in units of MeV

4. $\sigma^2(m,(\lambda\mu),T)$ of $U(3\mathcal{N}) \supset U(\mathcal{N}) \otimes [SU_T(3) \supset O_T(3)]$ in IBM-T (or IBM-3); here one has to use the $\hat{X}_3$ and $\hat{X}_4$ integrity basis operators of $SU_T(3) \supset SO_T(3)$,
5. $\sigma^2(m,\{f\})$ of $U(6\mathcal{N}) \supset U(\mathcal{N}) \otimes SU_{ST}(6)$ in IBM-ST (or IBM-4),
6. $\sigma^2(m,\{f\}ST)$ of $U(24) \supset U(6) \otimes [SU_{ST}(4) \supset SU_S(2) \otimes SU_T(2)]$ for $(2s1d)$ shell nuclei and similarly for $(2p1f)$ shell nuclei [also just $\sigma^2(m,\{f\})$],
7. $\sigma^2(m,T)$ of $U(2\mathcal{N}) \supset U(\mathcal{N}) \otimes SU_T(2)$ in shell model spaces,
8. $\sigma^2(\mathbf{m},T)$ and $\sigma^2(\mathbf{m},\mathbf{T})$ in shell model; $\mathbf{T} = (T_1, T_2, \ldots)$ with T_i being the isospin of m_i nucleons in a j_i orbit,
9. $\sigma^2(m,J)$ for $(j)^m$ system of fermions and $\sigma^2(m,L)$ for $(\ell)^m$ system of bosons [here, expansions in powers of $J(J+1)$ are possible as discussed in Chap. 13]. Similarly, though much more complicated, also for multi-j shell fermion and multi-ℓ shell boson systems [39].

Using the propagation equations one can calculate for each member of EGOEs, $\sigma^2(\Gamma)$ without H matrix diagonalization and therefore it is easy to obtain $\overline{\sigma(\Gamma)} = \sqrt{\overline{\sigma^2(\Gamma)}}$ where the bar denotes average over the appropriate EGOE ensemble. Figure 14.9 gives $\overline{\sigma_k}$, $k = \Gamma$ in 4 examples: (a) EGOE$(1+2)$ for spinless fermions with $\{H\} = h(1) + \lambda\{V(2)\}$ and 6 fermions in 12 sp states. Here $\{V(2)\}$ is GOE in two particle spaces with unit variance for the matrix elements. For the single particle energies defining $h(1)$ and other details, see Chap. 5. In the calculations $\lambda = 0.3$ and number of members is 50. The irreps k are the $h(1)$ basis states. (b) Shell model with k being shell model basis states for the $(2s1d)^{m=12,J=4,T=0}$ system

with H defined by ^{17}O single particle energies and a two-body interaction called KLS. See [38] for details and note that the shell model results can be viewed as the results for a typical member of EGOE(1 + 2)-JT. (c) BEGOE(1 + 2) for bosons with $\{H\} = h(1) + \lambda\{V(2)\}$ and 10 bosons in 5 sp states. Here $\{V(2)\}$ is GOE in two particle spaces with unit variance for the matrix elements. For the single particle energies defining $h(1)$ and other details, see Chap. 9. In the calculations $\lambda = 0.1$ and number of members is 20. The irreps k are $h(1)$ basis states. (d) BEGOE(1 + 2)-($sdg : L$) constructed for sdgIBM [17]. Here, in $\{H\} = h(1) + \lambda\{V(2)\}$, $V(2)$ preserves L. There are 32 two-body matrix elements defining $V(2)$ in sdgIBM and they are chosen to be independent Gaussian variables with zero center and unit variance. The k's in this example are the configurations defined by (m_s, m_d, m_g). Therefore, s, d and g boson single particle energies will not contribute to the k-variances; see Eq. (14.18). In calculating the number of widths, the dimensions $\binom{n_d+4}{4}\binom{n_g+8}{8}$ of the configurations (m_s, m_d, m_g) is taken into account. Calculations are for 15 bosons and number of members in the ensemble is 500. It is clearly seen from Fig. 14.9 that in all the examples the ensemble averaged fixed irrep widths, i.e. $\overline{\sigma_k}$, are nearly constant with respect to k and the fluctuation (∼5–10 %) in the widths $\overline{\sigma_k}$ is Gaussian distributed for fermion systems while it is asymmetric for bosons. Constancy of variances appear to be a generic property of EE (see also Chap. 12).

14.6 Results from EGOE(1 + 2)-s, EGOE(1 + 2)-π, BEGOE(1 + 2)-F and BEGOE(1 + 2)-$S1$ Ensembles

14.6.1 EGOE(1 + 2)-s *Results*

In Chap. 7 we have already shown that random interactions with EGOE(1 + 2)-**s** generate two important ordered structures: (i) spin $S = 0$ ground states; (ii) odd-even staggering in ground state energies. These features are also seen in EGOE(1 + 2)-J and EGOE(1 + 2)-JT [3]. Going beyond these, regularities with random interactions have been studies via pairing operator expectation values. In the eigenfunctions defined by the EGOE(1 + 2)-**s** Hamiltonian

$$H = h(1) + \lambda\left[\left\{V^{s=0}(2)\right\} + \left\{V^{s=1}(2)\right\}\right], \tag{14.19}$$

expectation values of the pairing Hamiltonian H_p given by Eq. (6.36) are calculated in a number of examples in [40]. In Fig. 14.10 results are shown for a 50 member EGOE(1 + 2)-**s** ensemble with 8 fermions ($m = 8$) in 8 orbits ($\Omega = 8$) and for $S = 0$ and 1. The exact results are compared with the EGOE formula given by Eq. (4.82) both with and without Edgeworth corrections. In this example $\lambda_c = 0.05$ and for this λ value we have (with $K = H_p$) for the K densities: ε_K, $|\gamma_1(K)| \sim 0$, $\sigma_K \sim 1.06$, $\gamma_2(K) \sim -0.33$ and $\langle K\rangle^{m,S} \sim 2.22$ for $S = 0$. Similarly, $\gamma_2(K) \sim -0.37$ and $\langle K\rangle^{m,S} \sim 2.00$ for $S = 1$. For $\lambda = 0.3 \gg \lambda_F$, we have

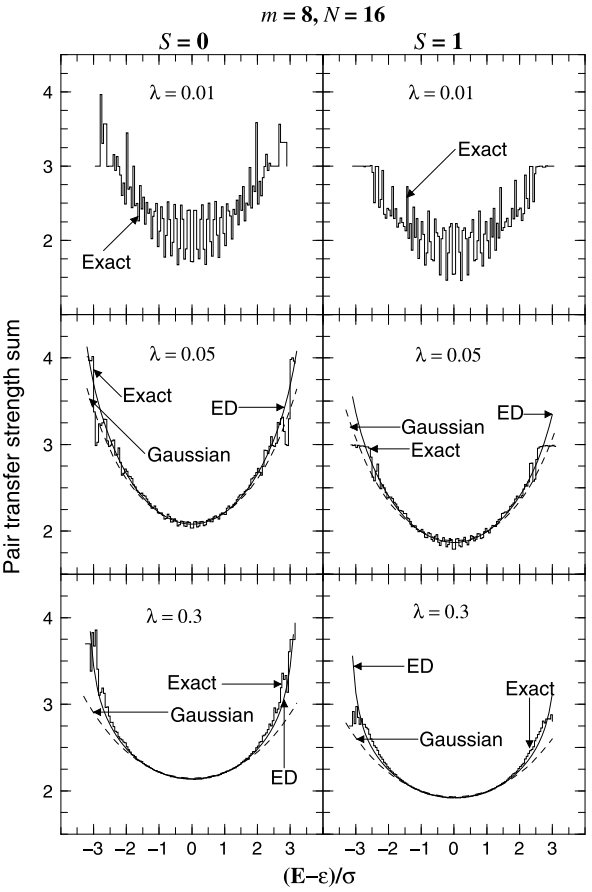

Fig. 14.10 Pairing expectation value or pair transfer strength sum $\langle PP^{\dagger}\rangle^{E} = \langle H_P\rangle^{E}$ vs $\hat{E} = (E-\varepsilon)/\sigma$ for a 500 member EGOE(1 + 2)-**s** ensemble with $\Omega = m = 8$ (number of sp states $N = 16$) and total spins $S = 0$ and 1; ε and σ are centroid and width of the eigenvalues E. Results (called 'exact' in the figure) are shown for various values of the strength λ of the two-body part of H; H is defined by Eq. (14.19). Results are compared with the EGOE formula given by Eq. (4.82) with Gaussian forms and also with Edgeworth corrected Gaussians (called ED in the figure)

$\gamma_2(K) \sim -0.44$ for $S = 0$ and -0.47 for $S = 1$. As seen from the figure, pair expectation values follow, in the chaotic domain ($\lambda \geq \lambda_c$) the simple EGOE law with little fluctuations. More importantly, at low energies the pair expectation value is large (still much smaller than the that for the pure pairing Hamiltonian) and then deceases as we go to the center (after that it will again increase as the space is finite). Also the expectation value in ground state domain for $S = 0$ is always larger than for $S = 1$. Thus, random interactions, even in the chaotic domain, exhibit stronger pairing correlations in the ground state region and they decrease as we go up in the energy. To probe pairing generated by random interactions further, one can use fixed seniority (v) partial densities $I^{m,v,S}$. Then, $f(v) = I^{m,v,S}(E)/I^{m,S}(E)$ gives the fraction of the intensity of the states with a given v in the eigenstate with energy E. For the random Hamiltonian given by Eq. (14.19), for $\lambda = 0.3$ in Fig. 14.10, $f(v)$ for $v = 0, 2, 4$ and 6 are 7 %, 33 %, 42 % and 18 % for $\hat{E} = -3$ and 12 %, 44 %, 37 % and 7 % for $\hat{E} = -3.1$. Thus in the ground state domain, although the pair expectation values are enhanced, the wavefunctions have relatively small strength for $v = 0$ states, i.e. they are not close to pure H_p eigenstates. This result is consistent

with the EGOE(1 + 2)-J and EGOE(1 + 2)-JT results obtained using nuclear shell model codes [3, 34]. Let us add that in [41], the splitting of sp energies was shown to play important role in EGOE(1 + 2)-J generating pair structure in low-lying states.

14.6.2 EGOE(1 + 2)-π *Results*

Experimental data on the parity of the ground states show that all known even-even nuclei have +ve parity ground states without any exception. In the compilation used in [4], there are 346 odd-A nuclei with A $>$ 120 where parity of ground states is known. The shell model space for these involve sp states with both parities. In the data it is seen that there are 182 nuclei with +ve parity ground states clearly identified and 164 nuclei with −ve parity. Similarly, there are 146 odd-odd nuclei (with A $>$ 120) with 68 of them having +ve parity ground states and the remaining having −ve parity. Thus, data shows preponderance of +ve parity ground states in even-even nuclei even when sp states of both parity are present in the shell model space appropriate for these and similarly, there is near equilibration of both parities for odd-A and odd-odd nuclei. Using shell model spaces $(f_{5/2}p_{1/2}g_{9/2})^{m_p,m_n}$, $(h_{11/2}s_{1/2}d_{3/2})^{m_p,m_n}$, $(f_{5/2}p_{1/2}g_{9/2})^{m_p}(g_{7/2}d_{5/2})^{m_n}$ and for many different values of proton (m_p) and neutron (m_n) numbers, EGOE(1 + 2)-J calculations have been performed in [34] and it is found that they generate ground states with parities having pattern almost close to that found in experimental data. Then, an important question is how to understand the shell model results using much simpler EE that include parity degree of freedom.

Towards this end, Papenbrock and Weidenmüller [42] used EGOE(1 + 2)-π ensemble introduced in Chap. 8 with $\tau \to \infty$, $\alpha = \tau$ and studied the probability (R_+) for +ve parity ground states over the ensemble for several (N_+, N_-, m) systems. Their numerical calculations showed considerable variation (18–84 %) in R_+. In addition, they gave a plausible proof that in the dilute limit [$m \ll (N_+, N_-)$], R_+ will approach 50 %. Combining these, they argued that the observed preponderance of +ve parity ground states could be a finite size (finite N_+, N_-, m) effect. However, for the general EGOE(1 + 2)-π considered in Chap. 8, it was shown in [43] that R_+ can reach 100 % by varying the α and τ parameters and we will turn to these results briefly.

For EGOE(1 + 2)-π with $\tau \sim 0$, clearly one will get $R_+ = 100$ % for even m (with $m \ll N_+, N_-$). Going beyond this, calculations have been carried out for a 200 member ensemble for $(N_+, N_-, m) = (6, 6, 6)$ and a 100 member ensembles for (8, 8, 5), (6, 6, 6), (6, 10, 4) and (6, 10, 5) systems using $\alpha = \tau$ and 1.5τ. The results are shown in Fig. 14.11. For $\alpha = \tau$, the results are as follows. For $\tau \lesssim 0.04$, we have $R_+ \sim 100$ % and then R_+ starts decreasing with some fluctuations between $\tau = 0.1$ and 0.2; τ is restricted to the realistic range of $\tau \leq 1$. It is seen that $R_+ \gtrsim 50$ % for $\tau \leq 0.3$ independent of (N_+, N_-, m) and then it decreases much faster reaching ∼30 % for $\tau = 0.5$ for $(N_+, N_-, m) = (6, 6, 6)$. For $m < (N_+, N_-)$, the decrease in R_+ is slower. If we increase α, we can easily infer that the width of the lowest +ve

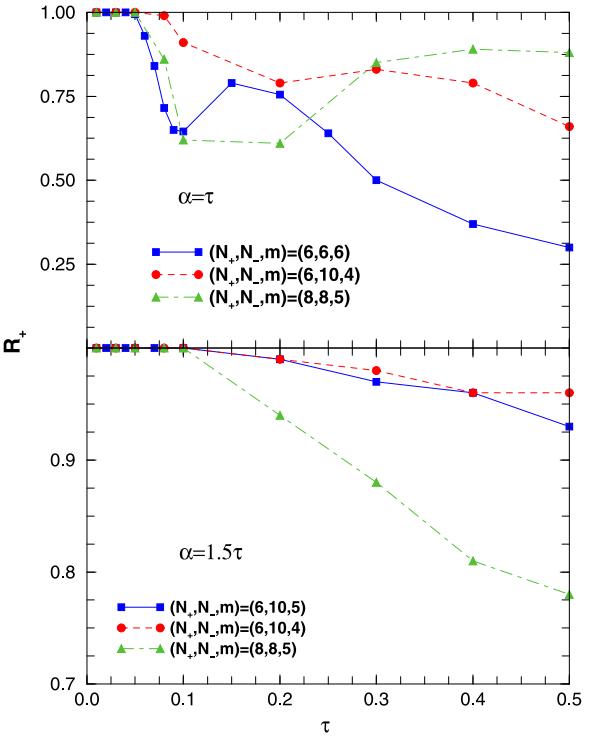

Fig. 14.11 Probability (R_+) for +ve parity ground states for various (τ, α) values and for various (N_+, N_-, m) systems in EGOE$(1+2)$-π. Figure is taken from [43] with permission from American Physical Society

parity (m_1, m_2) unitary configuration becomes much larger compared to the lowest $-$ve parity unitary configuration. Therefore with increasing α, R_+ is expected to increase and this is clearly seen in Fig. 14.11. Thus $\alpha \gtrsim \tau$ is required for R_+ to be large. A quantitative description of R_+ requires the construction of $+$ve and $-$ve parity state densities accurately in the tail region and this calls for more detailed analytical study of EGOE$(1+2)$-π.

14.6.3 Results from BEGOE$(1+2)$-F *and* BEGOE$(1+2)$-$S1$

Turning to BEGOE, in Chap. 10 some of the ordered structures generated by random interactions in BEGOE$(1+2)$-F are presented and they are: (i) $F = F_{max}$ ground states; (ii) natural F-spin ordering. In addition, just as in EGOE$(1+2)$-**s**, BEGOE$(1+2)$-F also generates ground states with relatively large value for the expectation value of the pairing Hamiltonian H_p; H_p is defined by Eq. (F.2). Expectation values $\langle H_p \rangle^{m,F,E}$ of the pairing Hamiltonian in the eigenstates generated by BEGOE$(1+2)$-F carry signatures of pairing. It is useful to note that, given the eigenvalues E_p of the pairing operator and eigenvalues E of the Hamiltonian operator, pairing expectation values are nothing but the centroids of the conditional density $\rho^{\Gamma}(E_p|E) = \rho^{\Gamma}(E_p, E)/\rho^{\Gamma}(E)$ defined over

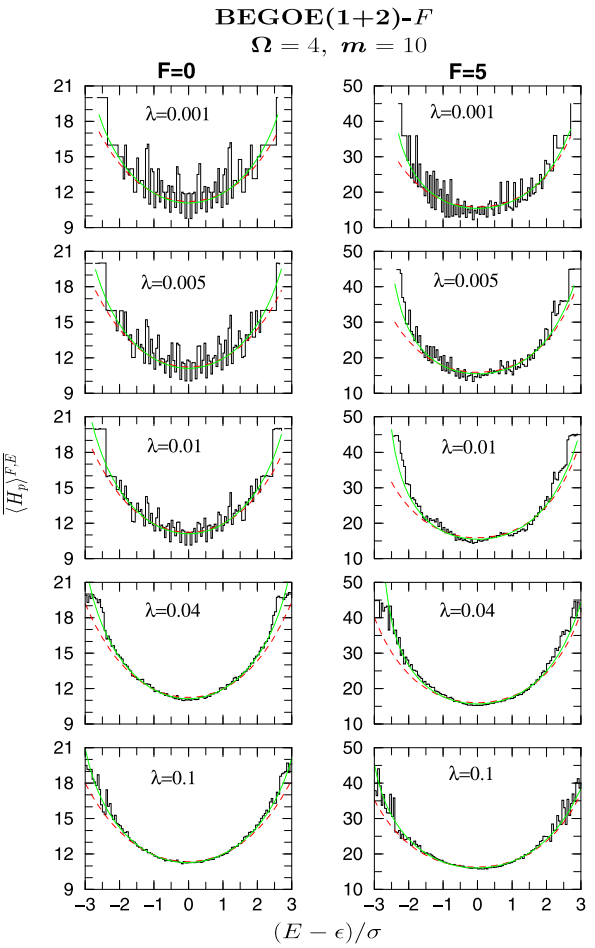

Fig. 14.12 Pairing expectation value $\langle H_P \rangle^{m,F,E}$ vs $\hat{E} = (E - \varepsilon)/\sigma$ for a 100 member BEGOE(1 + 2)-F ensemble with $\Omega = 4$ and $m = 10$ (number of sp states $N = 8$); ε and σ are centroid and width of the eigenvalues E. Ensemble results (histograms in the figure) are shown for various values of the strength λ of the two-body part of H; H is defined by Eq. (10.3) with $\lambda_0 = \lambda_1 = \lambda$. The sp energies are $\varepsilon_i = i + 1/i$ as used in Chap. 10. Results for $F = 0$ and 5 are compared with Eq. (4.82) with Gaussian forms (*red dashed curves*) and also with Edgeworth corrected Gaussians (*green continuous curves*)

fixed-$\Gamma = F$ spaces. Numerical results for a 100 member BEGOE(1 + 2)-F are shown in Fig. 14.12. Results are similar to those in Fig. 14.10. Firstly pairing expectation values are largest near the ground state. Secondly the EGOE formula, ratio of Gaussians as given by Eq. (4.82), is seen to apply to BEGOE(1 + 2)-F. Application of Eq. (F.9) shows clearly (see also Table F.1) that the maximum value of the H_p eigenvalues increases with F-spin for a fixed-m. The values are 28, 32, 34, 42, 48 and 60 for $F = 0$–5 respectively, for $\Omega = 4$ and $m = 10$. Numerical results in Fig. 14.12 also show that for states near the lowest eigenvalue (near the ground state) increases with F-spin. Thus random interactions preserve this regular property of the pairing Hamiltonian in addition to generating $F = F_{max}$ ground states as discussed in Sect. 10.1.4.

There are some preliminary investigations of regular structures generated by BEGOE(1 + 2)-$S1$ in [44]. As an example, shown in Fig. 14.13 are results for expectation values of the two pairing Hamiltonians $H_{\mathscr{P}}$ and H_P (see Sects. F.2.1

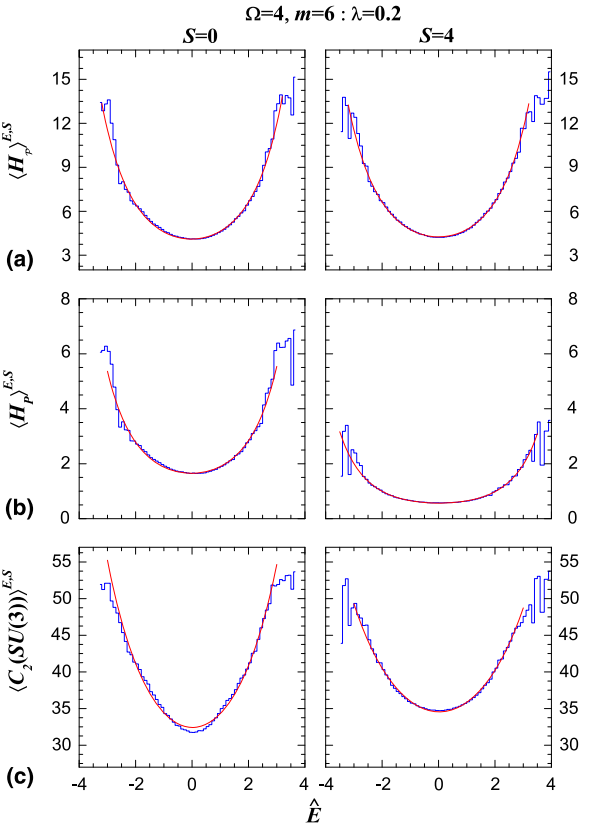

Fig. 14.13 Expectation values of the two pairing Hamiltonians $H_{\mathscr{P}}$ and H_P and $\hat{C}_2(SU(3))$ vs $\hat{E} = (E - \varepsilon)/\sigma$ for a 250 member BEGOE$(1+2)$-$S1$ systems with H defined by Eq. (10.17) and $(\Omega = 4, m = 6)$. Results are shown for spins $S = 0$ and $S = 4$. (**a**) expectation values of $H_{\mathscr{P}}$, (**b**) expectation values of H_P and (**c**) expectation value of $\hat{C}_2(SU(3))$. Ensemble averaged results are shown by histograms while (*red*) *continuous curves* are from theory (ratio of Edgeworth corrected Gaussians) given by Eq. (4.82)

and F.2.2) and also $\hat{C}_2(SU(3))$ in the eigenstates of the BEGOE$(1+2)$ Hamiltonian defined by Eq. (10.17). We have chosen the parameters in the region of chaos, i.e. $\lambda_0 = \lambda_1 = \lambda_2 = \lambda = 0.2$ so that fluctuations in the expectation values will be minimal. It is seen that the expectation values are largest near the ground states and then decrease as we move towards the center of the spectrum. The calculated results are in good agreement with the prediction that for boson systems also expectation values will be ratio of Gaussians. Results in the figure show that with repulsive pairing, ground states will be dominated by low seniority structure (small value for ω or $\omega_1 + \omega_2 + \omega_3$). In addition, results in Fig. 14.13c show that random interactions give ground states with large value for the expectation value of $\hat{C}_2(SU(3))$. Moreover, for the irrep $(m, 0) = (6, 0)$, we have easily $\langle \hat{C}_2(SU(3)) \rangle^{m=6,(6,0),S} = 54$ and from the figure one can then infer that ground states will be dominated by the $SU(3)$ irrep $(\lambda\mu) = (m, 0) = (6, 0)$. This result is of importance for IBM-3 model of atomic nuclei [21].

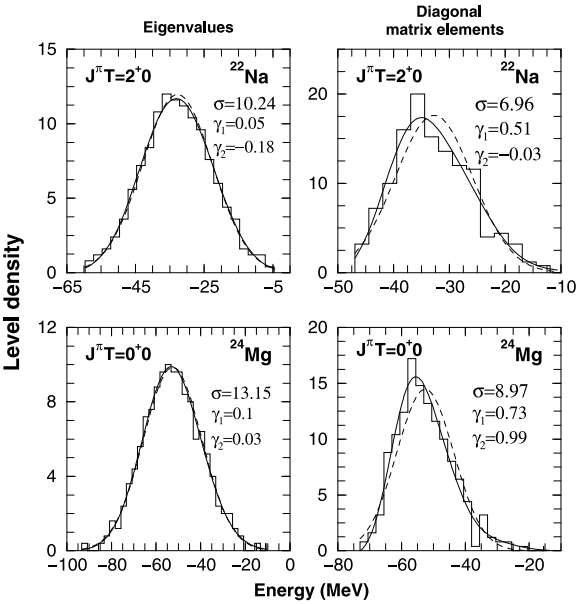

Fig. 14.14 Plot showing density of eigenvalues and density of diagonal matrix elements for the Hamiltonian matrices of ^{22}Na and ^{24}Mg nuclei obtained using nuclear shell model in $(2s1d)$ space. Values of the widths σ, skewness γ_1 and excess γ_2 are given in the figures. The units for σ are MeV. The centroid $E_c = -32.77$ MeV for ^{22}Na and -52.59 MeV for ^{24}Mg. Histograms are the exact results with bin size 2.5 MeV for all the examples. The *dashed curves* are the Gaussians with centroid E_c given above and width σ whose value is given in the figure. Similarly *continuous curves* are Edgeworth corrected Gaussians. Figure is taken from [45] with permission from Springer

14.7 Correlations Between Diagonal H Matrix Elements and Eigenvalues

Large number of numerical calculations have shown [46, 47] that the joint probability distribution $\rho(E, e_k)$ of the diagonal matrix elements e_k and eigenvalues E of a typical nuclear shell model H matrix is close to a bivariate Gaussian and this has its origin in a similar result valid more generally for EGOE$(1+2)$-J (or JT). Therefore the marginal densities $\rho(E)$ and $\rho(e_k)$ will be close to Gaussians with same centroids but different widths and the widths of the conditional densities $\rho(E|e_k)$ will be independent of e_k. These results have been used to derive a formula for the number of principal components and information entropy in wavefunctions as given in Chap. 5. The close to Gaussian form of $\rho(E)$ and $\rho(e_k)$ imply that the eigenvalues E and the diagonal elements of the H matrix (or equivalently the basis state energies) will be correlated. Flambaum et al. examined, for CeI, eigenvalue spectrum vs the spectrum generated by e_k [48] and they found a close correlation between the two spectra. As an example, density of eigenvalues and density of diagonal matrix elements for the Hamiltonian matrices of ^{22}Na and ^{24}Mg nuclei are

shown in Fig. 14.14. These distributions are compared with the Gaussian form ($\rho_{\mathscr{G}}$) and the Edgeworth (ED) corrected Gaussian form (ρ_{ED}). It is clearly seen that the eigenvalue distributions for the two nuclear examples are quite close to $\rho_{\mathscr{G}}$ while the densities of the diagonal matrix elements are, with some deviations, close to ρ_{ED}. These results reconfirm [45] that in the nuclear examples, the eigenvalues and the diagonal matrix elements of the H matrix are highly correlated and their distributions are close to Gaussian forms. In atomic examples much larger differences are found to exist [45] and this could be because atomic examples are much further from EGOE$(1+2)$-J. It should be added that, more recently Zhao et al. have argued [49, 50], using many EGOE$(1+2)$-J and EGOE$(1+2)$-JT numerical examples, that high correlation between eigenvalues and diagonal matrix elements is a much more a general phenomena. Using this, an extrapolation scheme was proposed by Zhao et al. [51, 52] for determining the energies of ground state and other low-lying states within nuclear shell model without diagonalizing huge matrices.

14.8 Collectivity and Random Interactions

Following the initial result of Bijker and Frank [2] that sdIBM with random interactions generate vibrational and rotational spectra, as shown in Fig. 14.2, there are many investigations within nuclear shell model (i.e. using fermion systems) to understand the origin of collective motion in atomic nuclei. To this end, studied using random interactions in some shell model spaces are: (i) predominance of prolate nuclear deformation [53]; (ii) origin of quadrupole collectivity in nuclei [54]; (iii) generation of pairing seniority structure and quadrupole vibrations and rotations [55]; (iv) generation of vibrational and rotational structure within the FDSM model which is a truncated version of the shell model [56]. Although numerical results do indicate that random interactions generate collectivities, there is no good analytical understanding yet. In an another interesting application, EGOE$(1+2)$-J and EGOE$(1+2)$-JT are used by some groups to identify important parts of the two-body interaction in the configuration-interaction shell model [53, 57]. Finally, it is also found in numerical calculations that random interactions in sdIBM of atomic nuclei generate strong correlations between energy levels generating many different regular structures such as preponderance of ground states with $L = 0^+$, an-harmonic vibrations, d-boson condensation, rotational motion and so on [58, 59].

In conclusion, results of various studies on regular structures generated by random interactions, discussed in some detail in this chapter, confirm the statement of Zelevinsky and Volya [3]: *Standard textbook ideas of the factors that form the low-lying structure of a closed self-sustaining mesoscopic systems are insufficient. The quantum numbers of the ground states and some regularities of spectra emerge not necessarily due to the corresponding coherent parts of the inter-particle interaction*.

References

1. C.W. Johnson, G.F. Bertsch, D.J. Dean, Orderly spectra from random interactions. Phys. Rev. Lett. **80**, 2749–2753 (1998)

2. R. Bijker, A. Frank, Band structure from random interactions. Phys. Rev. Lett. **84**, 420–422 (2000)
3. V. Zelevinsky, A. Volya, Nuclear structure, random interactions and mesoscopic physics. Phys. Rep. **391**, 311–352 (2004)
4. Y.M. Zhao, A. Arima, N. Yoshinag, Regularities of many-body systems interacting by a two-body random ensemble. Phys. Rep. **400**, 1–66 (2004)
5. D. Mulhall, Quantum chaos and nuclear spectra, Ph.D. Thesis, Michigan State University, East Lansing, USA (2002)
6. T. Papenbrock, H.A. Weidenmüller, Distribution of spectral widths and preponderance of spin-0 ground states in nuclei. Phys. Rev. Lett. **93**, 132503 (2004)
7. D. Kusnezov, Two-body random ensembles: from nuclear spectra to random polynomials. Phys. Rev. Lett. **85**, 3773–3776 (2000)
8. R. Bijker, A. Frank, Mean-field analysis of interacting boson models with random interactions. Phys. Rev. C **64**, 061303(R) (2001)
9. V.K.B. Kota, Random interactions in nuclei and extension of 0^+ dominance in ground states to irreps of group symmetries. High Energy Phys. Nucl. Phys. (China) **28**, 1307–1312 (2004)
10. C.W. Johnson, Random matrices, symmetries and many-body states (2011). arXiv:1103.4161
11. M.W. Kirson, J.A. Mizrahi, Random interactions with isospin. Phys. Rev. C **76**, 064305 (2007)
12. V.K.B. Kota, Interacting boson model applications to exotic nuclear structure, in *Recent Trends in Nuclear Physics—2012*, AIP Conf. Proc., vol. 1524 (2013), pp. 52–57
13. V.K.B. Kota, Transformation brackets between $U(N) \supset SO(N) \supset SO(N_a) \oplus SO(N_b)$ and $U(N) \supset U(N_a) \oplus U(N_b) \supset SO(N_a) \oplus SO(N_b)$. J. Math. Phys. **38**, 6639–6647 (1997)
14. F. Iachello, A. Arima, *The Interacting Boson Model* (Cambridge University Press, Cambridge, 1987)
15. F. Iachello, R.D. Levine, *Algebraic Theory of Molecules* (Oxford University Press, New York, 1995)
16. D.J. Rowe, F. Iachello, Group theoretical models of giant resonance splittings in deformed nuclei. Phys. Lett. B **130**, 231–234 (1983)
17. Y.D. Devi, V.K.B. Kota, sdg interacting boson model: hexadecupole degree of freedom in nuclear structure. Pramana—J. Phys. **39**, 413–491 (1992)
18. D.F. Kusnezov, Nuclear collective quadrupole-octupole excitations in the $U(16)$ $spdf$ interacting boson model, Ph.D. Thesis, Yale University, USA (1988)
19. G.L. Long, W.L. Zhang, H.Y. Li, E.G. Zhao, Sci. China, Ser. A, Math. Phys. Astron. **41**, 1296–1301 (1998)
20. V.K.B. Kota, Spectra and E2 transition strengths for $N = Z$ even-even nuclei in IBM-3 dynamical symmetry limits with good s and d boson isospins. Ann. Phys. (N.Y.) **265**, 101–133 (1998)
21. J.E. García-Ramos, P. Van Isacker, The interacting boson model with $SU(3)$ charge symmetry and its applications to even-even $N \approx Z$ nuclei. Ann. Phys. (N.Y.) **274**, 45–75 (1999)
22. V.K.B. Kota, $O(36)$ symmetry limit of IBM-4 with good s, d and sd boson spin-isospin Wigner's $SU(4) \sim O(6)$ symmetries for $N \approx Z$ odd-odd nuclei. Ann. Phys. (N.Y.) **280**, 1–34 (2000)
23. D. Mulhall, A. Volya, V. Zelevinsky, Geometric chaoticity leads to ordered spectra for randomly interacting fermions. Phys. Rev. Lett. **85**, 4016–4019 (2000)
24. Y.M. Zhao, A. Arima, K. Ogawa, Energy centroids of spin I states by random two-body interactions. Phys. Rev. C **71**, 017304 (2005)
25. V.K.B. Kota, K. Kar, Group symmetries in two-body random matrix ensembles generating order out of complexity. Phys. Rev. E **65**, 026130 (2002)
26. V.K.B. Kota, Regularities with random interactions in energy centroids defined by group symmetries. Phys. Rev. C **71**, 041304(R) (2005)
27. V.K.B. Kota, Group theoretical and statistical properties of interacting boson models of atomic nuclei: recent developments, in *Focus on Boson Research*, ed. by A.V. Ling (Nova Science Publishers Inc., New York, 2006), pp. 57–105

28. Y.M. Zhao, A. Arima, N. Yoshida, K. Ogawa, N. Yoshinaga, V.K.B. Kota, Robustness of regularities for energy centroids in the presence of random interactions. Phys. Rev. C **72**, 064314 (2005)
29. V.K.B. Kota, Two-body ensembles with group symmetries for chaos and regular structures. Int. J. Mod. Phys. E **15**, 1869–1883 (2006)
30. J.P. Elliott, Collective motion in the nuclear shell model. I. Classification schemes for states of mixed configurations. Proc. R. Soc. Lond. Ser. A **245**, 128–145 (1958)
31. J.P. Draayer, G. Rosensteel, $U(3) \rightarrow R(3)$ integrity-basis spectroscopy. Nucl. Phys. A **439**, 61–85 (1985)
32. Y. Akiyama, J.P. Draayer, A users guide to Fortran programs for Wigner and Racah coefficients of SU_3. Comput. Phys. Commun. **5**, 405–415 (1973)
33. R.U. Haq, J.C. Parikh, Space symmetry in light nuclei: (II). $SU(4)$ isospin-spin averages. Nucl. Phys. A **220**, 349–366 (1974)
34. Y.M. Zhao, A. Arima, N. Shimizu, K. Ogawa, N. Yoshinaga, O. Scholten, Patterns of the ground states in the presence of random interactions: nucleon systems. Phys. Rev. C **70**, 054322 (2004)
35. A. Volya, Emergence of symmetry from random n-body interactions. Phys. Rev. Lett. **100**, 162501 (2008)
36. P. Papenbrock, H.A. Weidenmüller, Origin of chaos in the spherical nuclear shell model: role of symmetries. Nucl. Phys. A **757**, 422–438 (2005)
37. V.K.B. Kota, R.U. Haq, *Spectral Distributions in Nuclei and Statistical Spectroscopy* (World Scientific, Singapore, 2010)
38. V.K.B. Kota, M. Vyas, K.B.K. Mayya, Spectral distribution analysis of random interactions with J-symmetry and its extensions. Int. J. Mod. Phys. E **17**(Supp), 318–333 (2008)
39. S.S.M. Wong, *Nuclear Statistical Spectroscopy* (Oxford University Press, New York, 1986)
40. M. Vyas, V.K.B. Kota, N.D. Chavda, One-plus two-body random matrix ensembles with spin: results for pairing correlations. Phys. Lett. A **373**, 1434–1443 (2009)
41. Y. Lei, Z.Y. Xu, Y.M. Zhao, S. Pittel, A. Arima, Emergence of generalized seniority in low-lying states with random interactions. Phys. Rev. C **83**, 024303 (2011)
42. T. Papenbrock, H.A. Weidenmüller, Abundance of ground states with positive parity. Phys. Rev. C **78**, 054305 (2008)
43. M. Vyas, V.K.B. Kota, P.C. Srivastava, One plus two-body random matrix ensembles with parity: density of states and parity ratios. Phys. Rev. C **83**, 064301 (2011)
44. H. Deota, N.D. Chavda, V.K.B. Kota, V. Potbhare, M. Vyas, Random matrix ensemble with random two-body interactions in the presence of a mean-field for spin one boson systems. Phys. Rev. E **88**, 022130 (2013)
45. M. Vyas, V.K.B. Kota, Random matrix structure of nuclear shell model Hamiltonian matrices and comparison with an atomic example. Eur. Phys. J. A **45**, 111–120 (2010)
46. J.B. French, V.K.B. Kota, Nuclear level densities and partition functions with interactions. Phys. Rev. Lett. **51**, 2183–2186 (1983)
47. V.K.B. Kota, K. Kar, Spectral distributions in nuclei: general principles and applications. Pramana—J. Phys. **32**, 647–692 (1989)
48. V.V. Flambaum, A.A. Gribakina, G.F. Gribakin, M.G. Kozlov, Structure of compound states in the chaotic spectrum of the Ce atom: localization properties, matrix elements, and enhancement of weak perturbations. Phys. Rev. A **50**, 267–296 (1994)
49. J.J. Shen, A. Arima, Y.M. Zhao, N. Yoshinaga, Strong correlation between eigenvalues and diagonal matrix elements. Phys. Rev. C **78**, 044305 (2008)
50. N. Yoshinaga, A. Arima, J.J. Shen, Y.M. Zhao, Correlation between eigenvalues and sorted diagonal elements of a large dimensional matrix. Phys. Rev. C **79**, 017301 (2009)
51. J.J. Shen, Y.M. Zhao, A. Arima, Lowest eigenvalue of the nuclear shell model matrix. Phys. Rev. C **82**, 014309 (2010)
52. J.J. Shen, Y.M. Zhao, A. Arima, N. Yoshinaga, New extrapolation method for low-lying states of nuclei in the sd and the pf shells. Phys. Rev. C **83**, 044322 (2011)

53. M. Horoi, V. Zelevinsky, Random interactions explore the nuclear landscape: predominance of prolate nuclear deformation. Phys. Rev. C **81**, 034306 (2010)
54. V. Abramkina, A. Volya, Quadrupole collectivity in the two-body random interaction. Phys. Rev. C **84**, 024322 (2011)
55. C.W. Johnson, H.A. Nam, New puzzle for many-body systems with random two-body interactions. Phys. Rev. C **75**, 047305 (2007)
56. Y.M. Zhao, J.L. Ping, A. Arima, Collectivity of low-lying states under random two-body interactions. Phys. Rev. C **76**, 054318 (2007)
57. C.W. Johnson, P.G. Krastev, Sensitivity of random two-body interactions. Phys. Rev. C **81**, 054303 (2010)
58. J. Barea, R. Bijker, A. Frank, Eigenvalue correlations and the distribution of ground state angular momentum for random many-body quantum systems. Phys. Rev. C **79**, 054302 (2009)
59. Y. Lei, Y.M. Zhao, N. Yoshida, A. Arima, Correlations of excited states for *sd* bosons in the presence of random interactions. Phys. Rev. C **83**, 044302 (2011)